Mathematical Model and Stability Analysis of the Electric Vehicle

BRAC UNIVERSITY
Inspiring Excellence

A Thesis Submitted to the Department of Electrical and Electronic Engineering of BRAC University

Authors

Srijon Talukder-11221063

Shafakat Nayem-12121104

Ajmaine Ibn Rahman-12121072

Supervised by

Dr. A. K. M. Abdul Malek Azad
Professor, Department of Electrical and Electronic Engineering
BRAC University, Dhaka

In partial fulfillment of the requirements for the degree of Bachelor of Science in Electrical and Electronic Engineering
Spring 2017
BRAC University

DECLARATION

We hereby declare that research work titled "*Mathematical model and stability analysis of electric vehicle*" is our own work. The work has not been presented elsewhere for assessment. The materials collected from other sources have been acknowledged here.

Signature of Supervisor	Signature of Authors
………………………………	……………………………….
Dr. A.K.M. Abdul Malek Azad	Srijon Talukder
	……………………………….
	Shafakat Nayem
	……………………………….
	Ajmaine Ibn Rahman

ABSTRACT

Light electric vehicles such as Tuk-Tuk, human haulers, and commuter bikes are gradually becoming a popular form of transportation in the cities as well rural areas of Bangladesh. A significant number of people of Bangladesh are directly or indirectly dependent upon this rickshaw-van pulling profession. This paper describes a research to modernize the pollution free rickshaw-van, aiming to improve the lifestyle and income of the rickshaw-pullers and reduce stress on the health of the pullers. The modernized rickshaw-van used in our experiment causes no carbon emission and thus it is eco-friendly. The electrically assisted rickshaw-van consists of torque sensor pedal in order to reduce the overuse of battery-bank. The control system assists the human power with motor and saves energy by reducing the overuse of motor. PV panel is installed on the rooftop of van to share the load power and a solar battery charging station is implemented to make the whole system completely independent of national grid. The paper describes the data obtained from field test to determine its performance, feasibility and user friendliness. The solar battery charging station is designed and its performance analysis is included as well. The hybrid "green" rickshaw-van was developed to save energy, use sufficient solar energy and make it a complete off grid solution. The thesis projects the theoretical functionality of the electric vehicles developed by CARC (Control & Applications Research Centre) through the development of mathematical model and henceforth the stability analysis which will help to ensure the reliability and ride comfort in the vehicles.

ACKNOWLEDGEMENT

We are thankful to our thesis supervisor Dr. A.K.M. Abdul Malek Azad, Professor, Dept. of Electrical and Electronic Engineering (EEE), BRAC University, for his sincere guidance for completion of the thesis. Regards to Project Engineers of CARC, Ataur Rahman and Research Assistant of CARC, Md, Jaber Al Rashid for their support throughout the whole thesis time span. We are also grateful to BRAC University for providing us the necessary apparatus for the successful completion of this project.

Contents

List of figures

List of tables

CHAPTER 1: Introduction

1.1 Introduction to Electric Vehicles

An **electric vehicle** (**EV**), also referred to as an **electric drive vehicle**, uses one or more electric motors for propulsion. An electric vehicle may be powered through a collector system by electricity from off-vehicle sources, or may be self-contained with a battery or generator to convert fuel to electricity. EVs include road and rail vehicles, surface and underwater vessels, electric aircraft and electric spacecraft. Electric vehicles have always been the center of fascination and the topics of research and development among common people and the scientists since 1827, when the Slovak-Hungarian priest Anyos Jedlik built the first crude but viable electric motor, provided with stator, rotor and commutator. After one year he used that motor in a small car. However, development of electric vehicles have been conferred since 1827 and still the development is not enough in this aspect as electric vehicles has gone through newly evolved technologies and efficiency level are ought to be increased maintaining different techniques. Mathematical models were developed from different perspectives of different aspects such as control systems, energy conversion and conservation etc. In the light of that, ***Control and Applications Research Centre (CARC)*** has conducted research on the electric vehicles that is electrically assisted rickshaw vans used for public transportation and perform door to door services in our country. The thesis group of ours have been given task of finding the mathematical model of this electric vehicle which was modified by CARC introducing torque sensing mechanism , position control and speed control loop in the vehicle system which has stabilized the vehicle with accordance of performance. We also are to do stability analysis of this torque sensor based electric vehicle and perform MATLAB simulation in order to analysis the electric vehicle in the theoretical perception.

1.2 Electric Vehicle Considered for Mathematical Model

In the meantime, CARC has developed gradually three tri wheeler electric vehicles such as human haulers, ambulance and cargo vehicle which were torque sensor pedal and PV support equipped electrically assisted electric vehicles.

Figure 1.1 Vehicle considered for mathematical model

Ride comfort was ensured in the vehicle by installing 4 springs under the seats. The vehicles were designed to reduce human effort by utilizing torque sensor, electric motors and increase the performance and efficiency of the system. The vehicles can practically be availed in rural areas where normal human haulers, ambulance or cargo are not available. Not only that, the concept of solar charging station and easy battery swapping techniques have also been introduced. Under normal conditions the vehicles can pick speed as normal grid charged electric vehicles can run.

1.3 Motivation

The slow-speed, muscle driven tri-wheeler is often blamed to be the cause of traffic jam and road accidents in Dhaka, where the city roads hardly have three lanes for cars. The vehicle uses muscular energy to drive and as a result, immense physical strain is involved in this occupation. The earning of the pullers compared to the physical strain involved is low. As mentioned earlier, a huge number of people are relying on rickshaw or rickshaw-van pulling profession, it is necessary to improve technologically in order to advance the living standard. The motivation for working on this research and development program has been originated from the observation that a substantial modernization in this sector will not only improve the living standard of a huge number of people involved in rickshaw pulling, but also improve the quality of life of upper and lower-middle income group people. The electrically assisted rickshaw-van will relieve the pullers from extreme physical exhaustion by assisting them electrically using torque sensor, which will limit the over-use of battery bank. Solar panel will help in sharing the load power and solar battery charging station will be used to charge the batteries instead of using power from national grid. Thus, CARC has been making and developing the technology for efficient use of renewable resources and making the system completely independent of national grid. Our purpose of this research that has been entrusted to us by CARC is to make the vehicles theoretically approachable and define the vehicles in equations and doing the stability analysis by thorough simulation process.

CHAPTER 2

Overview of the Whole System with Components

2.1 Introduction

The most common transportation vehicle in Dhaka city is rickshaw. Most of the people like to ride on this for which day by day it becomes the first choice as a public transportation. As Bangladesh is an under developed country, most of the people of this country are underprivileged. Therefore, significant number of people chooses their profession as a rickshaw puller. For the first time in Bangladesh Beevatech Limited had developed a motorized rickshaw-van which has a multiple input i.e. throttle and torque sensor pedal under the supervision of Control and Applications Research Centre (CARC) of BRAC University. As the government has disapproved commercialization of such motorized vehicle due to consumption of electricity from the already overloaded grid, our motive is to find a solution to conserve power for such green electric rickshaw-van with the use of PV panel, torque sensor pedal and solar battery charging station. The vehicle that we considered in our mathematical model has a brushless DC gear motor, four 12V 25Ah sealed lead acid batteries connected in series, a controller unit, a throttle, main power key, emergency motor stopper, traditional front wheel brake and an extra rear wheel break, charge controller, charge indicator and other components [2]. The details of all the components are mentioned in the following sections. Here is the skeleton view of the vehicle which we consider for our mathematical model is shown in Fig 2.1.

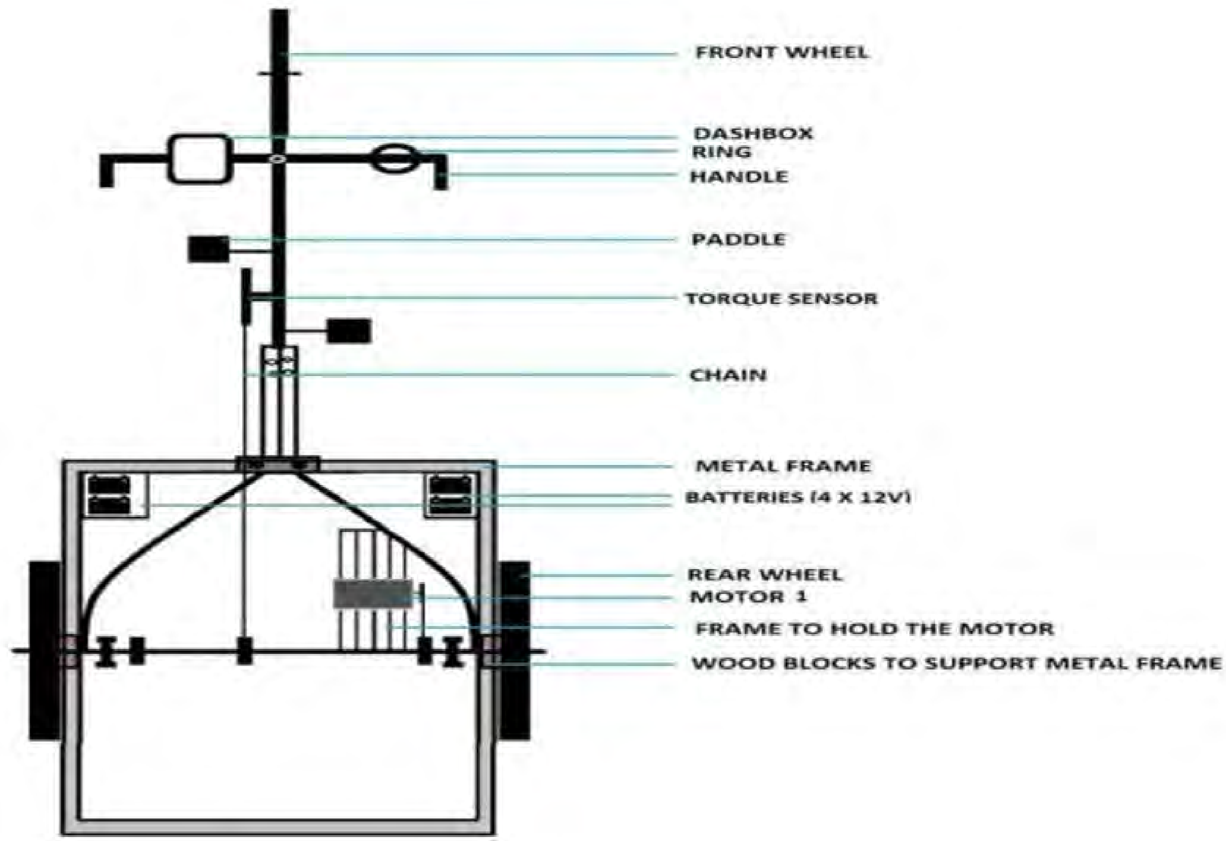

Figure 2.1 Skeleton View

2.2 Components considered for mathematical model

2.2.1 The Batteries

In the vehicle that we are considering, four sealed lead-acid batteries are used, which are connected in series. The dimension of each battery is 16.5 × 17.5 × 12.6 cm. Each of the battery is 12V, 25 Ah rechargeable which supplies 48 Volts to the BLDC motor. The batteries are placed under both the seats as shown in Fig 2.1. If we fully charge each of the battery it shows 12.7 volts across their terminals and 50.8 volts together as we connect the batteries in series [2].

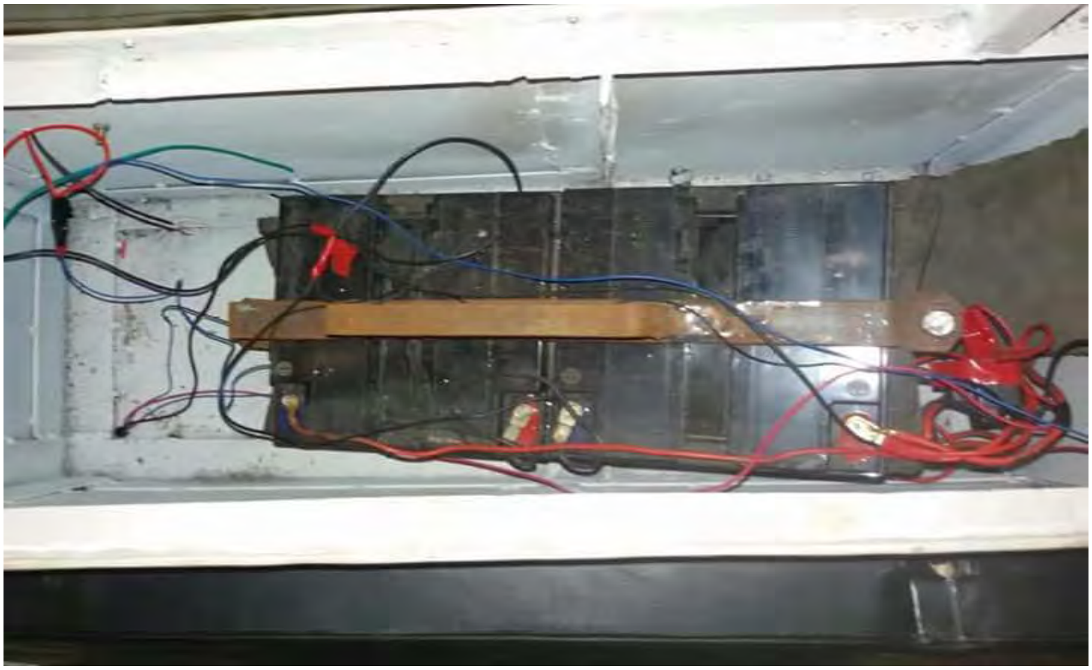

Figure 2.2 Two batteries

2.2.2 The Motor

The vehicle that we are considering, uses a brushless DC gear motor which has a, which has a power of 500 Watt and 500-550 rpm speed. This motor has a rated current and voltage of 13.4A and 48V which is attached with the main frame. It is mounted under the seat as shown in Fig 2.3. As this produces more torque per watt that's why it is very preferable for such kind of vehicles which linearly decreases as velocity decreases.

Figure 2.3 BLDC Motor

2.2.3 The Motor Controller Unit

In our vehicle a controller box is used. This box integrates all the necessary electrical components which are used to make the motor run properly. The motor controller unit has the following connections:

Connections :

- Motor Hall sensor
- Throttle/ Handle
- Battery
- Speed limiting cable
- Reverse switch
- Power lock
- Motor phase cable

We can clearly identify the connection from figure 2.4.

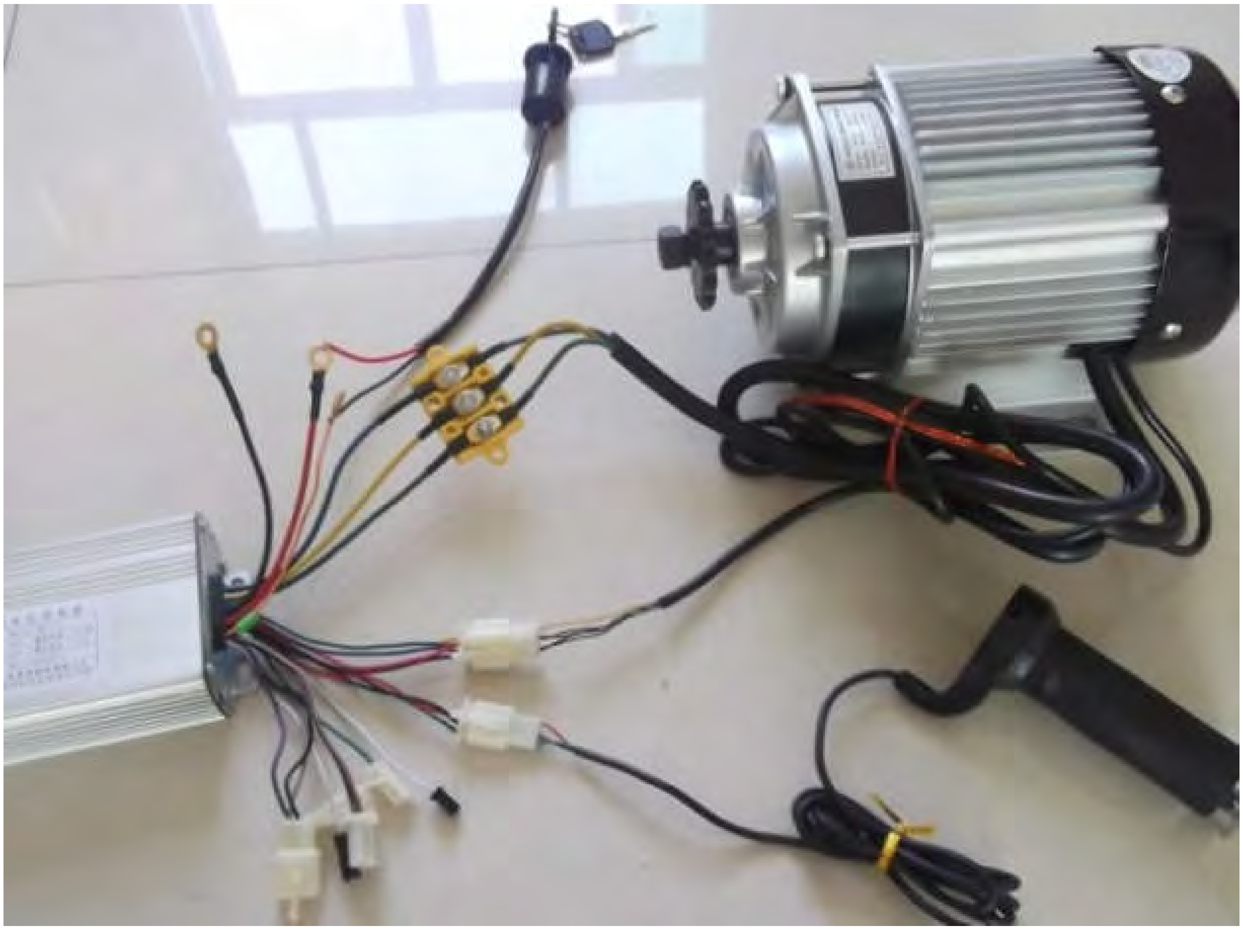

Figure 2.4 The Motor Controller Unit Connections

The following figure shows a clearer view for the identification of the motor controller unit wires.

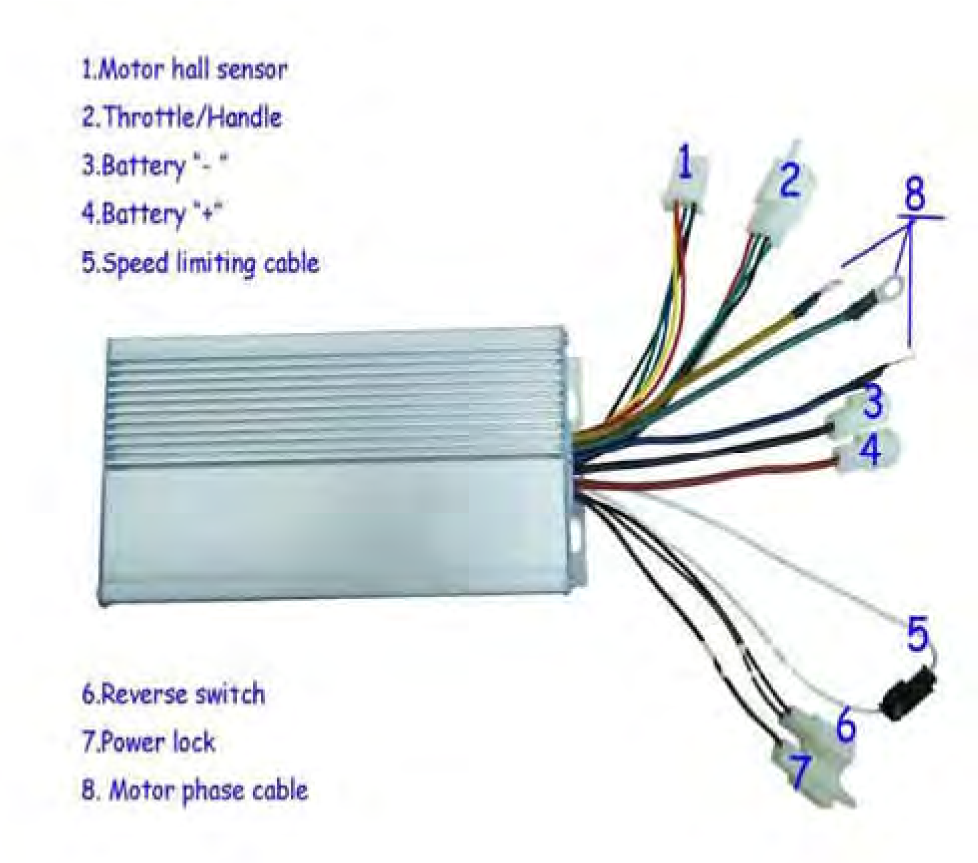

Figure 2.5 The Motor Controller Unit wiring

From the above figures the motor controller unit wiring is explained which is used for our vehicle.

2.2.4 The Throttle

The system of the vehicle has been designed as multiple inputs and one of them is throttle. To control the speed of the vehicle there is a huge impact of throttle. A throttle shown in Fig. 2.4 is a specially designed potentiometer. It has a biasing voltage of 5V which is provided by the motor controller unit. Its output voltage depends on the angle of the throttle. The motor speed increases as the output voltage increases. The motor starts when it gets 1.4 volts from the throttle and when the output voltage is 3.5 volt the motor rotates at its maximum speed [2].

Figure 2.6 The Throttle

2.2.5 The Torque Sensor

To measure and record the torque of a rotating system, torque sensor is highly preferable. To operate from the DC source it needs a biasing voltage of 5 volt and the voltage output is linear with the applied torque, within its operating region. The output voltage increases when the torque increases. The speed of the motor is directly proportional to the output voltage. The sensor was built in such a way that it could be fixed in any pedal driven electric vehicle. [2]. In our case the torque sensor takes input from the pedal torque and it converts mechanical torque into electric output. Fig 2.5 shows the torque sensor pedal that has been installed in vehicle which we consider for our mathematical model.

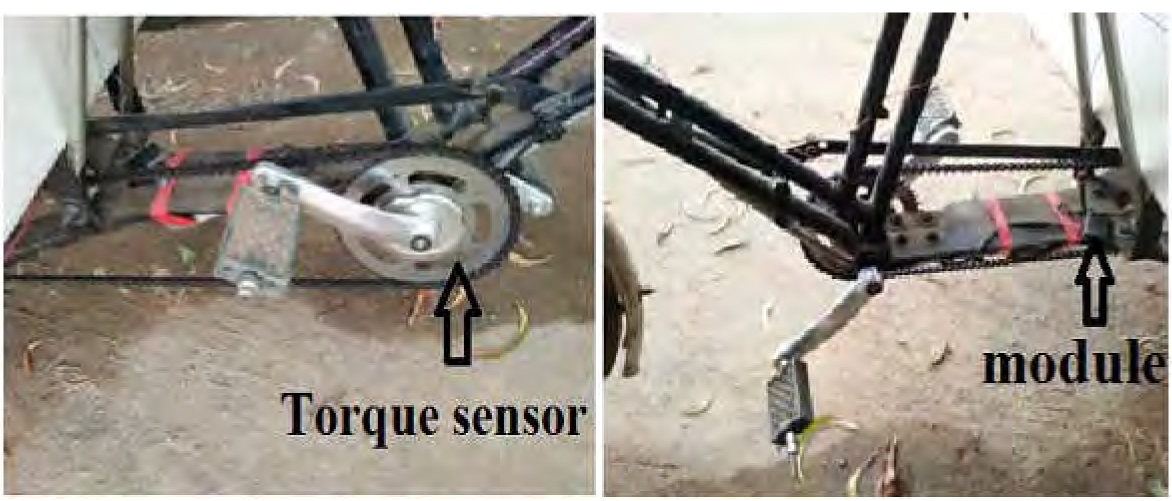

Figure 2.7 Torque sensor

Features of Torque Sensor [2]:

- Brush/Brushless motor controllers are applicable for it.
- Like a common chain wheel crank , its hardware can be installed.
- It has a sensor/sensor-less motor type electrical system.
- Aluminum alloy made body.
- Provides instant response while pressure is applied on pedal and pedaling is stopped.
- It reduces the pressure of pedaling.
- We got around 18 to 96 times from each crank rotation.
- Magnet ring integrated with multi-pole improving greatly the precision of signal.
- Sampling time in case of digitalization.
- The system has a good protection seal over water and dirt.

Technical Parameter Data of torque sensor [2]:

- V_{cc} = 5.15 V (+/- 0.15V)
- Output, linear, zero-start, 0.5~4.5V
- Output torque >15N-m
- Delay time < 50ms

2.2.6 Torque sensor pedal

As the vehicle has been designed as multiple inputs, here is another input the torque sensor pedal. The pedal torque works as the input of the system with torque sensor as the sensing components. Since the torque sensor has inertia so it generates the output and the signal processing module converts the mechanical energy to the voltage signal. This voltage signal energy works as the input signal of the electrical control system of the vehicle. It was made in such a way that it could be suitable in any tri or bicycle. Few mechanical modifications are required when it will be fixed in tri-wheeler like reshaping the main pedal axis ends etc. The Fig 2.6 shows the torque sensor pedal when implemented and installed into the electric vehicle [2].

Figure 2.8: Torque sensor pedal

2.2.7 Gear Train

A gear train is a mechanical system to determine the ratio of the rotational speed of two or more gears. Gear train works like an amplifier in a electromechanical system. Depending the number of teeth it amplifies the output which is used for mechanical transmission. In consideration of two gears one is drive gear and another one is driven gear. In general if the drive gear, which comes from the rotational force of engine and motor is higher than the driven gear the latter will turn more quickly and vice versa. To determine the gear ration we have to consider the number of teeth of driven gear and drive gear and set them into the following formula.

$$\text{Gear Ratio} = \frac{\text{No of teeth of Driven Gear}}{\text{No of teeth of Drive Gear}}$$

For our vehicle,

Number of teeth of the pedal (drive gear) =48

Number of teeth of the axle (driven)=10

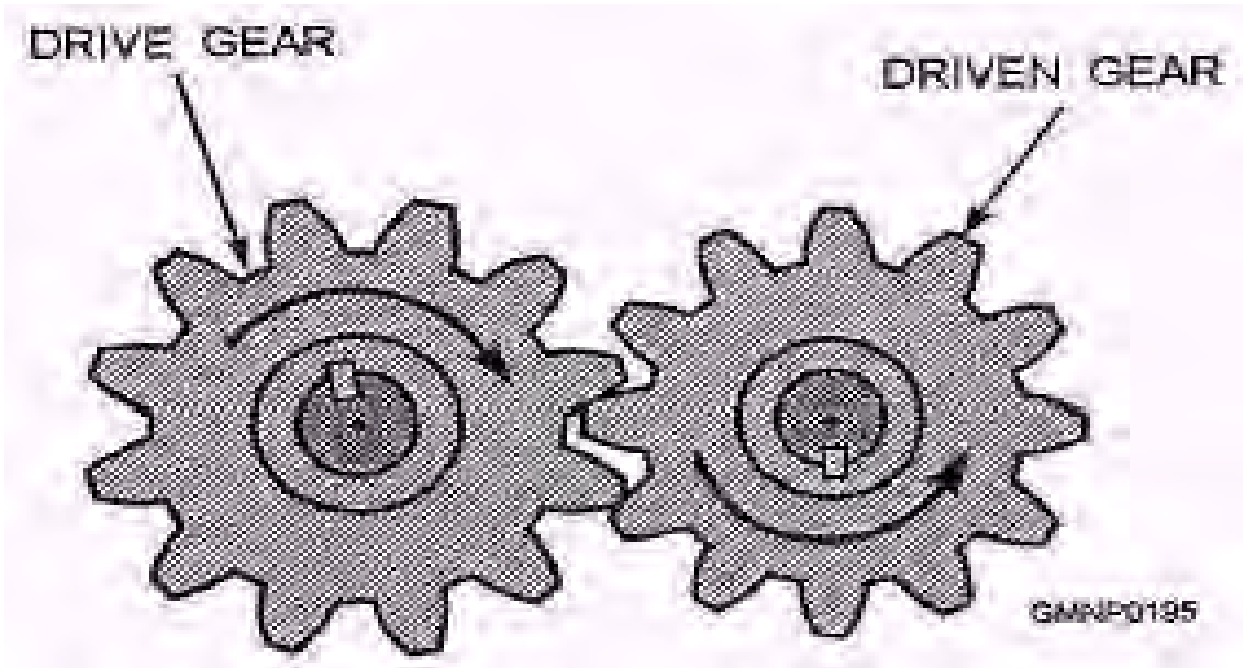

Figure 2.9 Gear Train

2.3 Conclusion

The electric vehicle that we are considering has got many other components installed in it, which are necessary to run the vehicle. For the mathematical model, those components are not required. We are only considering the electric and mechanical components which are needed for the mathematical model.

CHAPTER 3: Developing Mathematical Model

3.1 Introduction

In order to develop a mathematical model, we need to build up a schematic of the physical system first from which the mathematical interpretation will be done. Mathematical model can be derived using two methods-

a) Transfer functions in the frequency domain

b) State equations in the time domain

In any case, the first step to derive a mathematical model is to apply fundamental physical laws of science and engineering [1]. For instance, in case of modeling electrical networks, Ohm's laws and Kirchhoff's laws are applied. For mechanical system, we used Newton's laws as fundamental guiding principle [1]. In our thesis, we used the first of the two aforementioned methods for mathematical model. The model shaped as transfer function relates the input of the system to its output response. The reason for selecting the method is to represent the inputs, output and the system distinctly and separately. According to Nise (2015), a system represented by differential equation is difficult to model as a block diagram. Thus here comes the idea of Laplace transformation, with which input, output and the system can be represented individually. Not only will that, relationship between them will become algebraic.

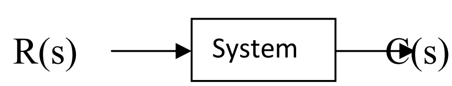

Where R(s) is reference input and C(s) is output represented in frequency domain.

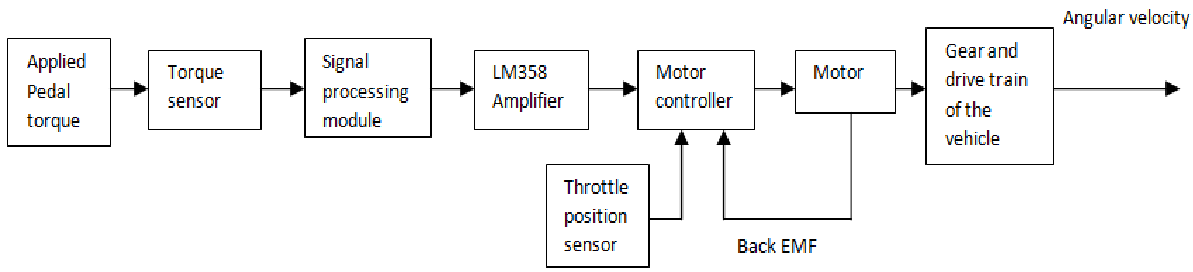

Figure 3.1 Overall gist of the operation

3.2 Block build up and explanations

From the first hand observation of the structure and operation of the vehicle and keeping the electrical, mechanical and electro-mechanical components used for the mathematical modeling in mind, we tried to build up a schematic of the vehicle and it is as follows,

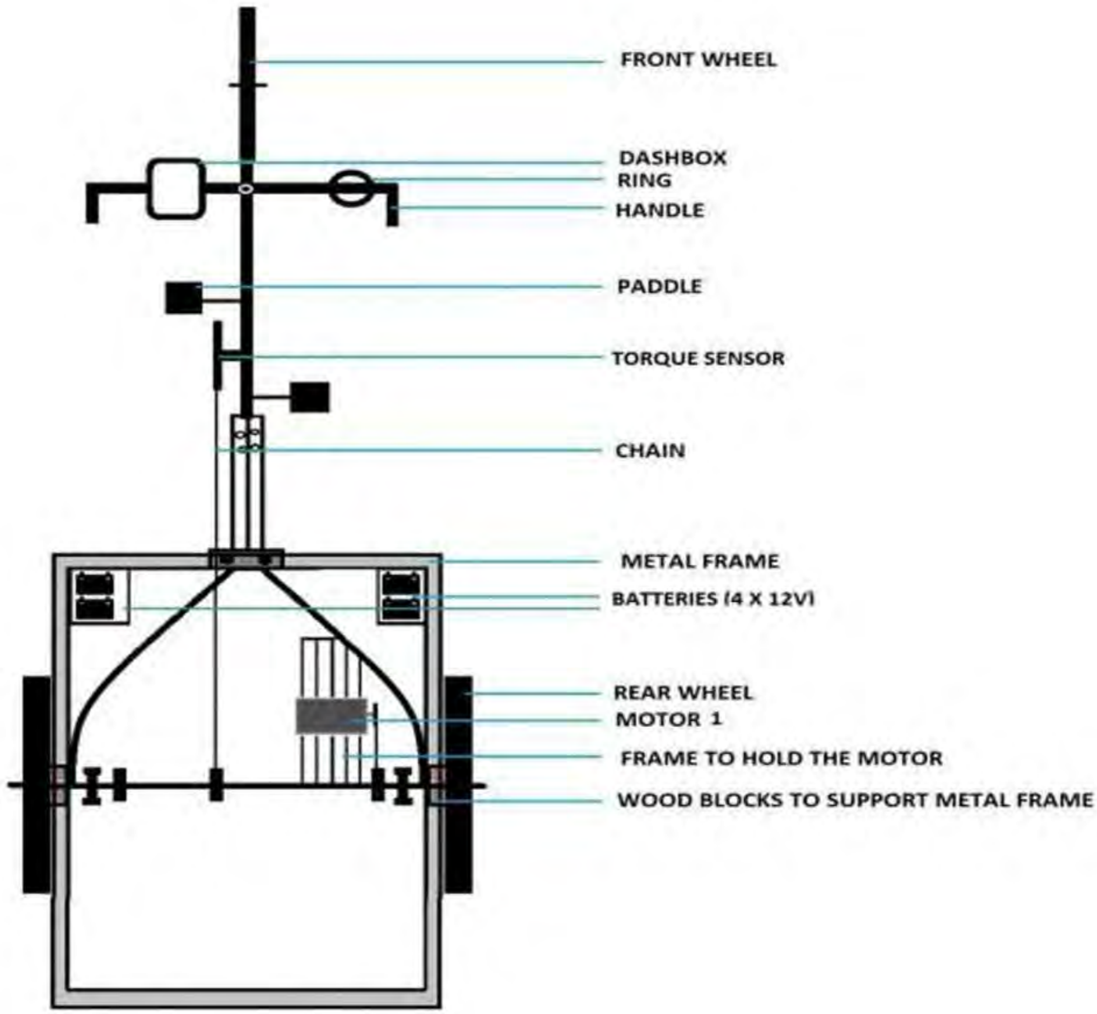

Figure 3.2 Schematic of the electric vehicle

3.2.1 Inputs and outputs of the system

The figure 3.1 describes the operation of the vehicle. When the rider starts pedaling, torque sensor converts the mechanical energy as pedal torque into electrical signal and feed the voltage after amplification of the signal. There is another input to the system which is throttle. Throttle located at the right handle bar acts as a rotary potentiometer. Depending on the angle of the throttle, the generated voltage is fed to the motor through motor controller.

As a result, the shaft of the motor rotates, which later rotates the axle of the rear wheels. Then we get the angular velocity of the wheels as well as linear displacement of the vehicle.

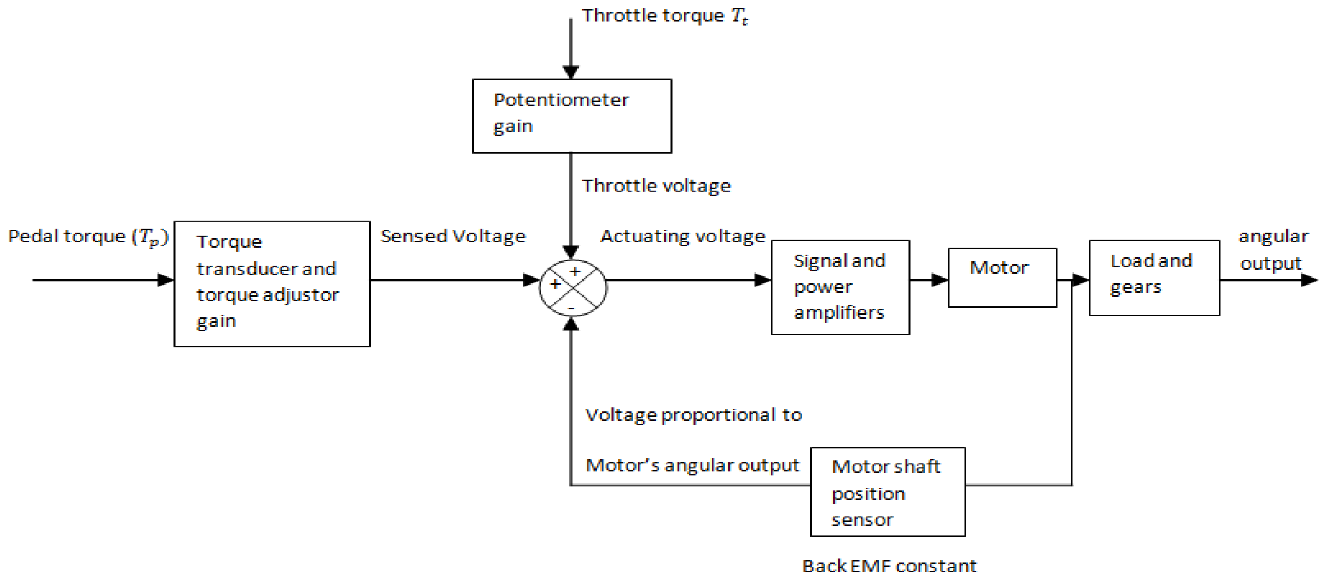

Figure 3.3 Functional block diagram of the system

3.3 Mathematical representation of the system

From figure 3.2 mathematical representation of the system has been determined from the identification of the electrical and mechanical functionality of block subsystems. Block by block analysis has been done as the following.

3.3.1 Torque sensor voltage from the Pedal torque T_P:

Torque sensor or torque transducer is means to convert the mechanical input (torque) to electrical signal. This is done by sensor attached in the crank set and a signal processing module is used to serve the purpose. Biasing voltage of torque sensor is 5 volts and it generates output voltage corresponding to the torque applied to the particular crank set [2]. The voltage output is linear with the applied torque. The parameter data of the torque sensor is given below:

- V_{CC}= 5.15 V (+/- 0.15 V)
- Output linear, zero start, 0.5~4.5 V
- Output torque >15 Nm

Figure 3.4 Torque sensor pedal and signal processing module

Since the relationship between torque input and produced voltage is linear, the proportionality of the torque-to-voltage can be assumed. To get maximum output of 4.5 V, at least 15 Nm applied torque is required. Then the proportional constant could be

$$k_p = \frac{4.5}{15} = 0.3 \text{ V/Nm}$$

The output voltage generated from the torque sensor and module was reduced to 60% by the developers of the vehicle [2] [3]. This purpose was fulfilled by the torque adjustor circuit. An LM358 amplifier was used after voltage division. The amplifier gave maximum output of 3.6 V when a voltage of +5 V supplied [3]. Thus, amplifier gain becomes 1.38. Maximum gain of 1.26 was used by [2] . For the torque sensor, the block diagram and numerical representation can be shown as following:

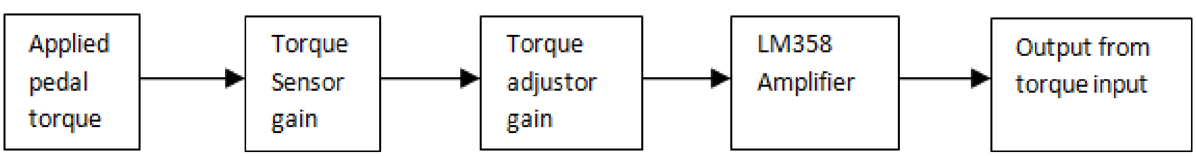

Figure 3.5 Block diagram of torque input

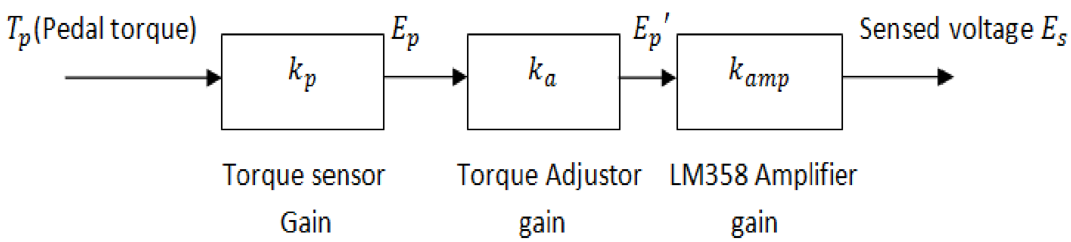

Figure 3.6 Mathematical representation of the torque input

Where,

$k_p = 0.3$

$k_a = 0.6$

$k_{amp} = 1.26$

3.3.2 Throttle Input:

As for throttle input, input torque T_t has been introduced. Throttles are generally used to control the speed of the motor. It is a rotary potentiometer with spring attached internally. A specific biasing voltage V_{CC} is supplied to the throttle from the motor controller unit and gives output as voltage corresponding to the angle (θ_t) of the throttle. Internal circuit diagram of the throttle is given in figure 3.5

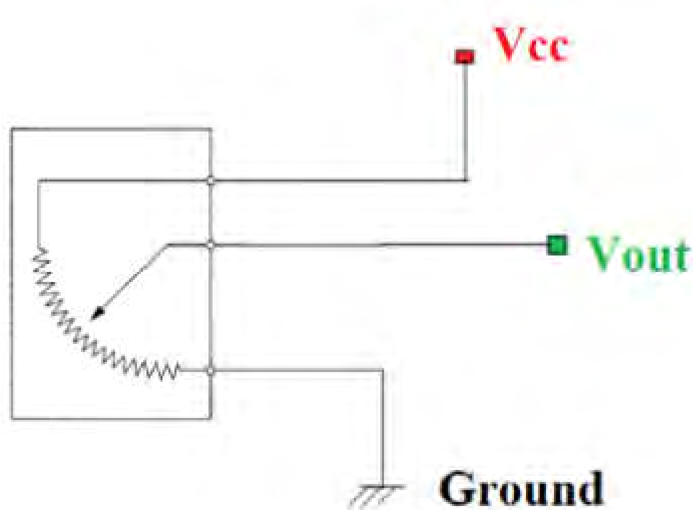

Figure 3.7 Diagram for a Throttle Position sensor

Throttle is the simplest electromechanical system [4]. Figure 3.6 shows how the throttle potentiometer works in the following:

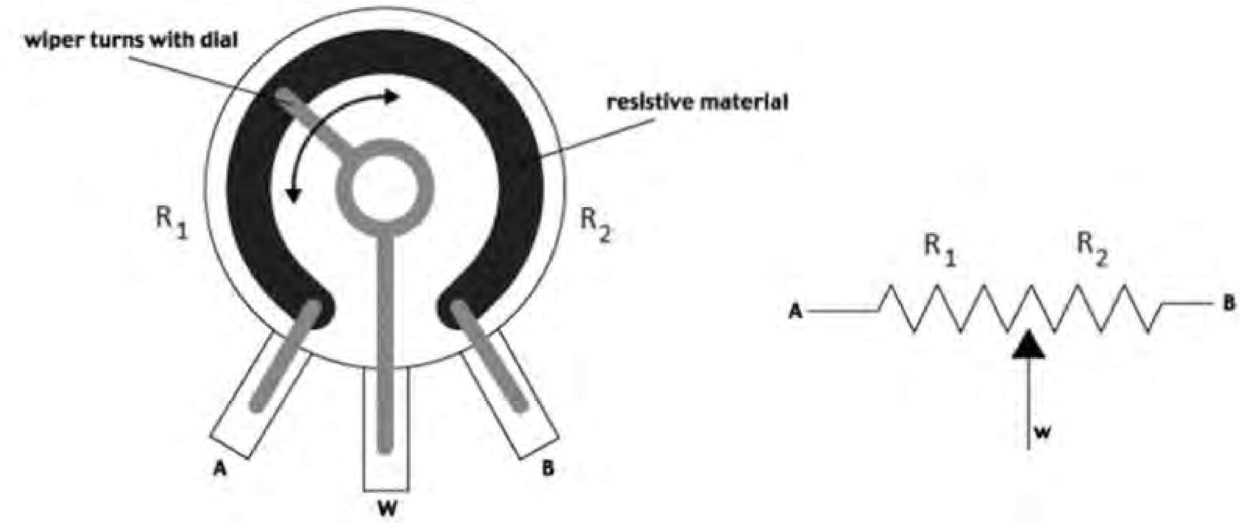

Figure 3.8 Rotary potentiometer

An arc of resistive material is there between the point A and B. the wiper W is a conductive material based on which the resistive value as well as the voltage output of potentiometer changes.

Let,

The resistance between A and wiper W : R_1

The resistance between W and B: R_2

Total resistance between A and B, $R_{total} = R_1 + R_2$

The voltage output increases at clockwise rotation. That means,

At point A, $\theta_t = 0$

At point B, $\theta_t = \theta_{tmax}$

R_1 and R_2 vary linearly with θ_t between the two end points as shown in figure 3.7 [4].

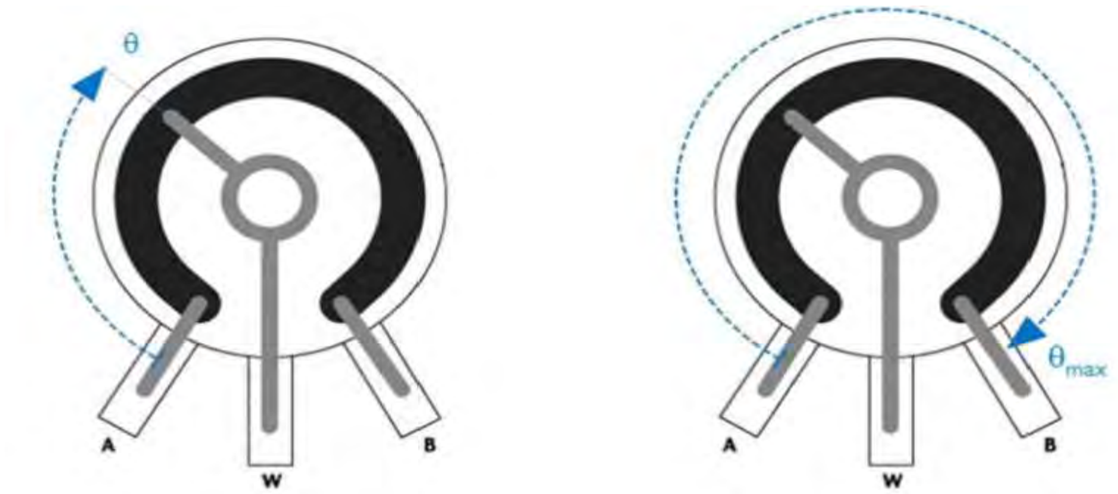

Figure 3.9 Resistance value changes according to angle

According to figure 3.9, we can write,

$R_1 = \frac{\theta_t}{\theta_{tmax}} R_{total}$ .... (1)

In order to sense the angular position of the throttle, consider the following equivalent circuit of the device:

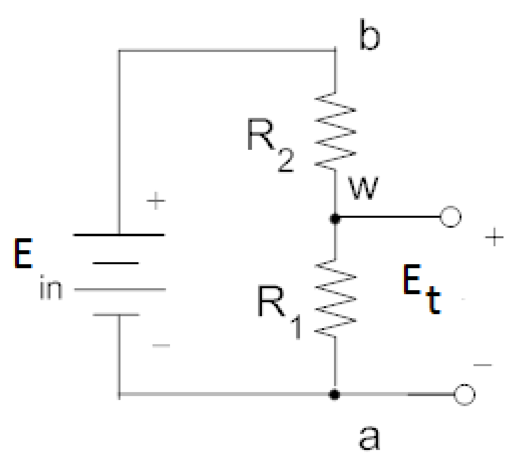

Figure 3.10 Equivalent circuit of the throttle potentiometer

Based on the throttle position (wiper position),

Throttle output voltage, $E_t = \frac{R_1}{R_{total}} E_{in}$,using voltage divider rule.

Substituting with (1) , we obtain,

$$E_t = \frac{\frac{\theta_t}{\theta_{tmax}} R_{total}}{R_{total}} E_{in}$$

$$\Rightarrow E_t = \frac{\theta_t}{\theta_{tmax}} E_{in}$$

$$\Rightarrow \frac{\theta_t}{E_t} = \frac{\theta_{tmax}}{E_{in}} \quad \text{..........(2)}$$

Considering the spring which tends to rotate back to its original position and in terms of torque input to the throttle,

$T_t = k_s \theta_t$, using Hooke's Law.

Where, k_s is a spring constant.

Substituting with equation (2), the equation yields as following,

$$E_t = \frac{k_s \theta_t}{k_s \theta_{tmax}} E_{in}$$

$$E_t = \frac{T_t}{T_{tmax}} E_{in}$$

$\frac{T_t}{E_t} = \frac{T_{tmax}}{E_{in}} = k_{throttle}$, which is a throttle constant.

Throttle technical information:

Some parameters of throttle used by [2],[3] was identified as following:

Working voltage: +5 V dc

Voltage output: 0.8-4.2 V

Degrees rotation angle: $0° - 70°$ ~ 0-1.22173 radian

Weight: 80 g

Throttle Constant, $k_{throttle}$:

From Hooke's law,

$$T_t = k_s\theta_t$$

$$\frac{\theta_t}{T_t} = \frac{1}{k_s} \text{ ……………………………………………………..(3)}$$

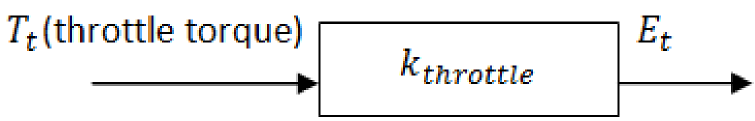

Figure 3.11 Block diagram for throttle

For potentiometer gain, from (2) and (3) we find,

$$\frac{E_t}{T_t} = \frac{E_t}{\theta_t} * \frac{\theta_t}{T_t}$$

$$\frac{E_t}{T_t} = \frac{\theta_{tmax}}{E_{in}} * \frac{1}{k_s} = \frac{\theta_{tmax}}{k_s E_{in}}$$

To rotate at maximum (70 degree~1.22173 rad), assumed maximum exerted force on throttle,

$$F_{max} = .150kg * 9.81m\ s^{-2} = 1.4715\,N$$

Multiplying by radius (r=0.5 in ~ 0.0127 m) of the throttle, we get,

$$T_{tmax} = 1.4715N * 0.0125m = 0.018\,Nm$$

Maximum throttle output voltage, $E_{tmax} = 4.2\ V$

Maximum angle deflection, $\theta_{tmax} = 1.22173$ rad

Spring constant, $k_s = \frac{\theta_{tmax}\ T_t}{E_t E_{in}} = \frac{1.22173*0.018}{5*4.2} = 0.001$ Nm/rad

$\frac{E_t}{T_t} = 244.346$, throttle gain which gives maximum throttle output voltage.

3.3.3 Motor and vehicle: circuits and dynamics

Throttle and torque sensor voltage adds into motor controller. Electrical behavior and mechanical dynamics of the motor can be described by the block diagram of the motor in figure 3.12.

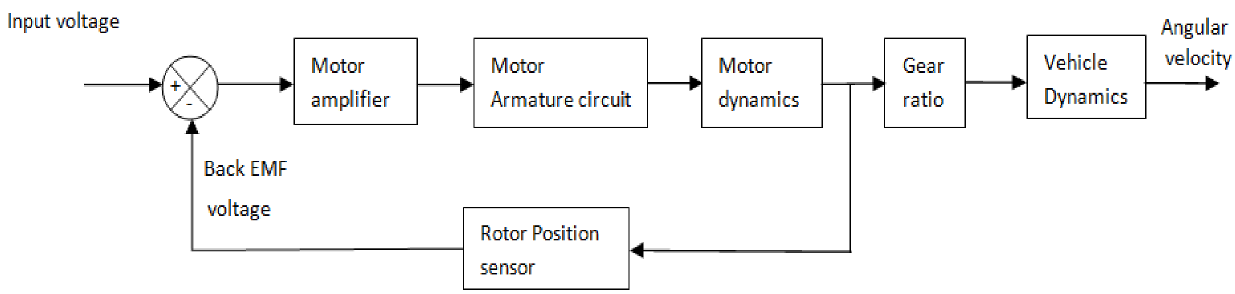

Figure 3.12 Functional block diagram of the motor

Motor circuit:

Electromechanical schematic diagram of the motor is shown in figure 3.11

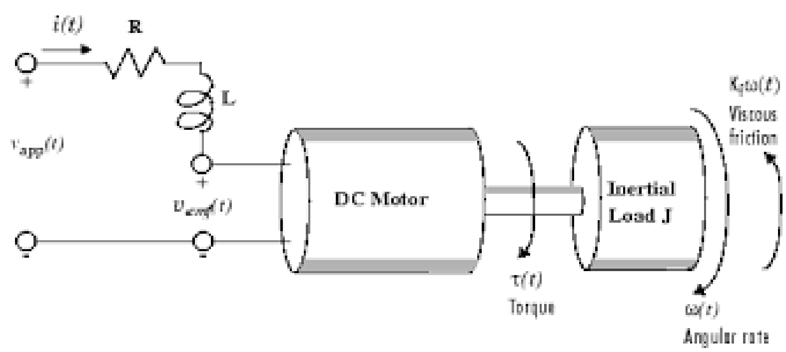

Figure 3.13 Schematic of the BLDC motor

From figure 3.11 electrical behavior of the motor can be understood [5] :

$$L_a \frac{di_a}{dt} + R_a i_a + E_b = k_m(E_s + E_t)$$

Using Laplace transformation assuming zero initial conditions, we get,

$$L_a s I_a + R_a I_a + E_b = k_m(E_s + E_t)$$

Here,

L_a= Armature inductance

I_a=Armature current

R_a=Armature resistance.

E_b=Back EMF voltage

E_s,E_t= Torque sensor voltage and throttle output voltage accordingly.

k_m=motor amplification constant

Therefore, transfer function for the motor armature circuit would be,

$$\frac{I_a}{k_m(E_s + E_t) - E_b} = \frac{1}{L_a s + R_a}$$

Back EMF voltage E_b is linearly proportional to the motor shaft angular velocity ω_m [5].

So, $E_b = k_b \omega_m$, k_b=back EMF constant

Motor and vehicle dynamics:

Analogies can be created between electrical and mechanical systems. It can be created by comparing torque-velocity relationship (such as $T(t) = J\frac{d\omega(t)}{dt}$) among mechanical components to current-voltage relationship (such as $v(t) = Ri(t)$) among electrical components [1].Here , torque is compared to current and velocity is to voltage. In this process,

Spring (k) is analogous to inductor (L).

Viscous damper (B) is analogous to resistor (R)

And mass/inertia (M/J) is compared to capacitor (C)

Thus, summing the torque/forces from the perspective of velocity resulting differential equations becomes analogous to node analysis. Using this idea, we tried to create an analogous circuit for the dynamics of the vehicle in consideration in figure 3.14

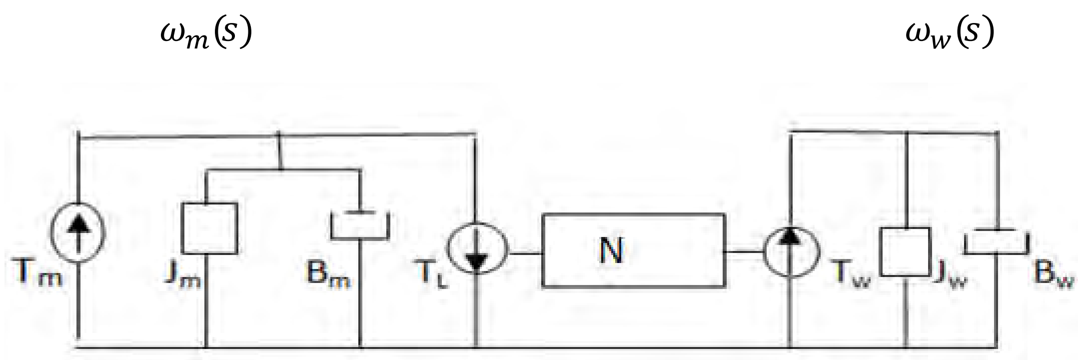

Figure 3.14 T-i analogous circuit for motor and vehicle dynamics

From the above figure we can find the motor dynamics equation in Laplace transformation assuming zero initial conditions.

$T_m(s) = J_{\ m} s\omega_m(s) + \ + B_m\omega_m(s) + \ T_L(s)$ .... (a)

Where,

T_m=motor torque

J_m=motor inertia

B_m=viscous damping co-efficient of motor

T_L=Load torque of the motor

Load torque produces wheel torque (T_w) after gear transmission.

Gear ratio in terms torque and velocity, $N = \frac{T_w}{T_m} = \frac{\omega_m}{\omega_w}$

$$\omega_w = \frac{\omega_m}{N}$$

Hence, for vehicle dynamics, without considering the resistance torque [5], we get,

$$T_L(s) * \ N \ = \ T_w = J_b s\omega_w(s) + \ B_w\omega_w(s)$$

$=> \quad T_L(s) = \frac{1}{N}[J_b s\omega_w(s) + B_w\omega_w(s)]$………………. (b)

J_b=Vehicle body Inertia

B_w=viscous damping co-efficient of wheels

Combining (a) and (b) ,

$$T_m(s) = J_m s\omega_m(s) + + B_m\omega_m(s) + \frac{1}{N}[J_b s\omega_w(s) + B_w\omega_w(s)]$$

From the perspective of motor, using gear transmission ratio, the equation finally yields,

$$T_m(s) = J_m s\omega_m(s) + + B_m\omega_m(s) + \frac{1}{N^2}[J_b s\omega_m(s) + B_w\omega_m(s)]$$

The transfer function in terms of motor torque, we get,

$$\frac{\omega_m(s)}{T_m(s)} = \frac{1}{\left(J_m + \frac{J_b}{N^2}\right)s + \left(B_m + \frac{B_w}{N^2}\right)} = \frac{1}{J_{eq}s + B_{eq}}$$

$$J_{eq} \rightarrow \left(J_m + \frac{J_b}{N^2}\right)$$

$$B_{eq} \rightarrow \left(B_m + \frac{B_w}{N^2}\right)$$

Furthermore, motor torque T_m has a linear relationship with armature current I_a. Hence, $T_m = k_t I_a$

$\frac{T_m}{I_a} = k_t$=motor torque constant

Finally, in figure 3.15, mathematical block diagram of the motor can be shown.

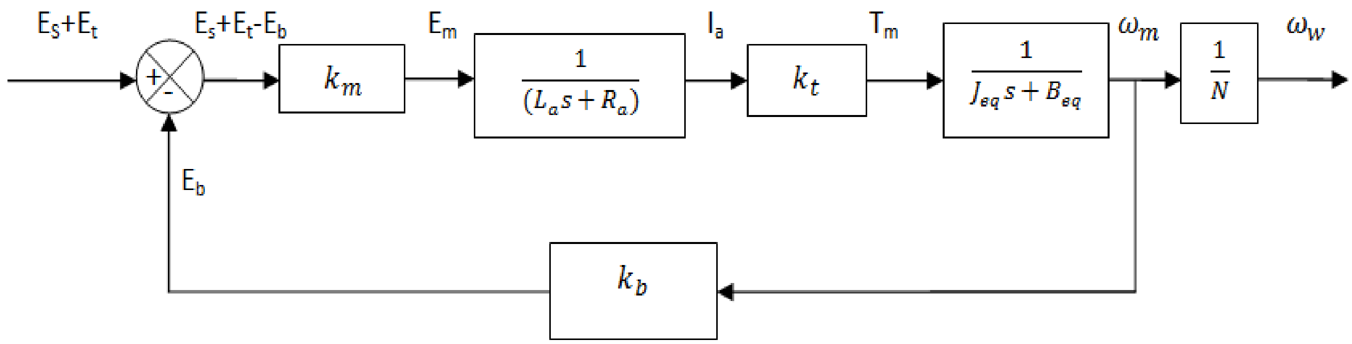

Figure 3.15 Electromechanical representations of the motor and vehicle dynamics

Motor electrical and mechanical parameters:

Motor parameters were identified from a Nanotec™ BLDC motor [6]. The parameters are given in the following:

Table 3.1: Motor parameter table

Nominal output	660 W
Nominal torque	2.10 Nm
Peak torque	6.30 Nm
Nominal voltage	48 V
Speed	3000 RPM
Torque constant, k_t	0.117 Nm/A
Resistance, R	0.07 ohm
Inductance,L	0.0001 H
Rotor inertia , J_m	0.00024 kgm^2
Viscous damping, B_m	0.008 Nms/rad
Back EMF constant,k_b	0.15 V/rad/s
Motor amplifier gain, k_m	48

As for the inertia acting on the wheel, the wheel has a cylindrical radius [7] and thus, estimating for m=250 kg load and radius r=13 inch~0.3302 m,

$$J_b = \frac{1}{2} m\, r^2 = 0.5 * 250 * 0.33\ 02^2 = 13.63\, kgm^2$$

ω_m at rated speed=3000 RPM~314.16 rad/s

At 70% efficiency of motor, $\omega_w = 314.16 * \frac{1}{0.70} = 448.8$ rad/s

As well as, $B_w = \frac{250*9.81*0.330\ 2}{448.8} = 1.8$ Nm/rad/s

$$J_{eq} = J_m + \frac{J_b}{N^2} = 0.0024 + \frac{13.63}{0.7^2} = 27.82\, kgm^2$$

$B_{eq} = B_m + \frac{B_w}{N^2} = 0.008 + \frac{1.8}{0.7^2} = 3.68$ Nm/rad/s

3.3.4 Mathematical model of the overall system

Combining the block diagrams from figure 3.6, 3.11 and 3.15, we obtain the final mathematical block diagram of the system.

From figure 3.6, substituting all the constants $k_p k_{\ a}$ & k_{amp} for k_{pedal} ,

$$k_{pedal} = k_p * k_a * k_{amp}$$

From figure 3.11,

$$k_{throttl\ e} = \frac{\theta_{tmax}}{k_s E_{in}}$$

and from figure 3.15,

$$E_u = E_s + E_t - E_b$$

Finally the block diagram for the full system in figure 3.16

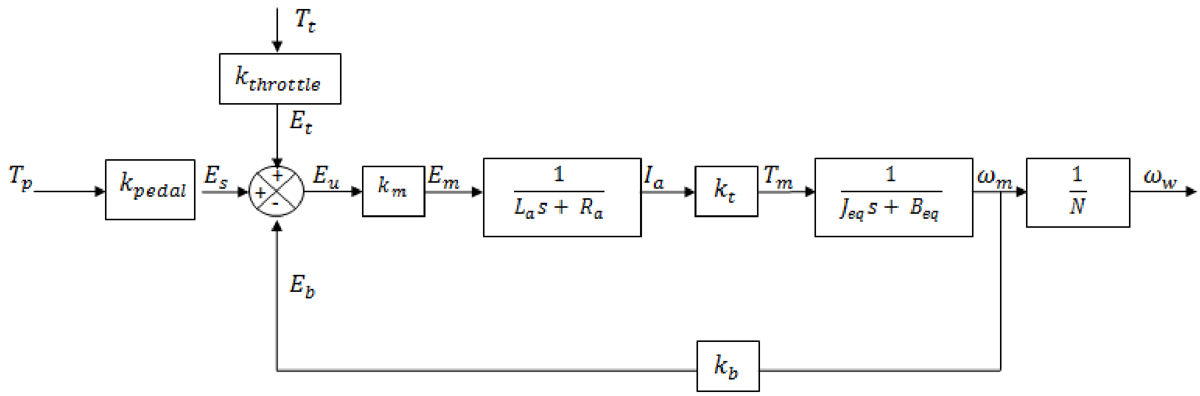

Figure 3.16 Mathematical block diagram of the full system

Derivation of final equation

Using superposition principle,

1) When T_p active, $T_t = 0$

   a)

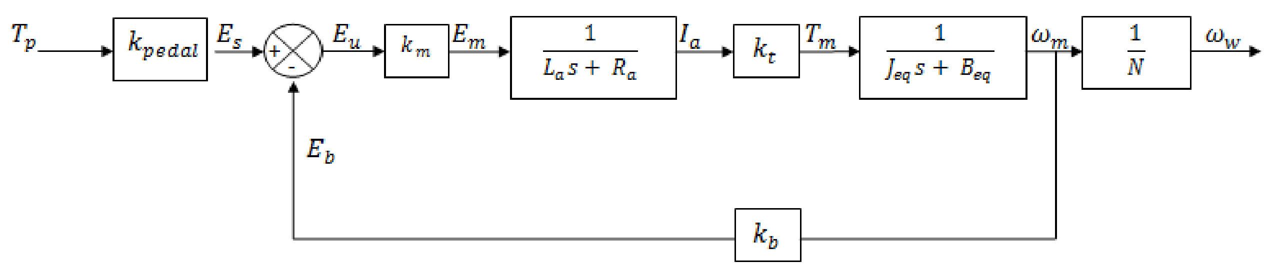

Figure 3.17 Block diagram for only pedal input

b) Using block diagram manipulation technique, figure 3.15 can be changed as following:

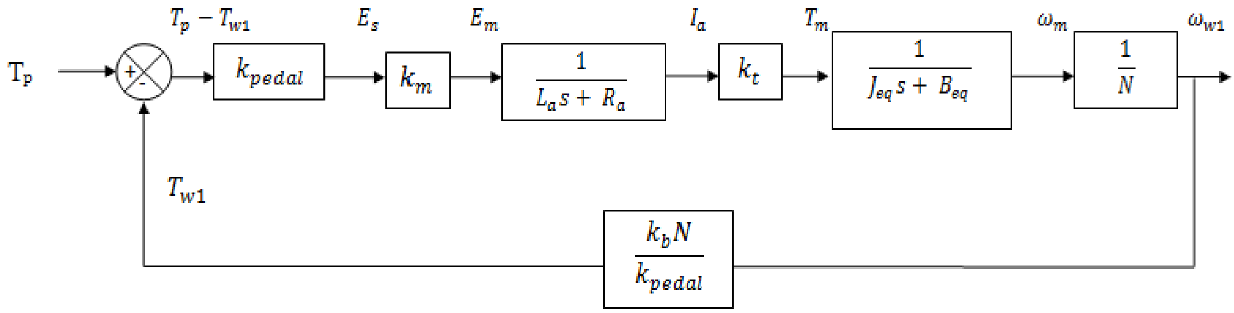

Figure 3.18

[N.B. Please notice that, the output of the feedback is a torque element of which, input is wheel angular velocity (ω_{w1}). To support the argument,

$$\frac{T_{w1}}{\omega_{w1}} = \frac{k_b N}{k_{pedd}} = \frac{\frac{k_b \omega_m}{\omega_{w1}}}{k_{pedd}}$$

$T_{w1} = \frac{k_b \omega_m}{k_{pedd}} = \frac{\frac{E_b}{E_s}}{T_p} = \frac{E_b}{E_s} T_p$; of which, unit is Nm (Newton meter), input is wheel angular velocity and so it is definitely a wheel torque output]

c)

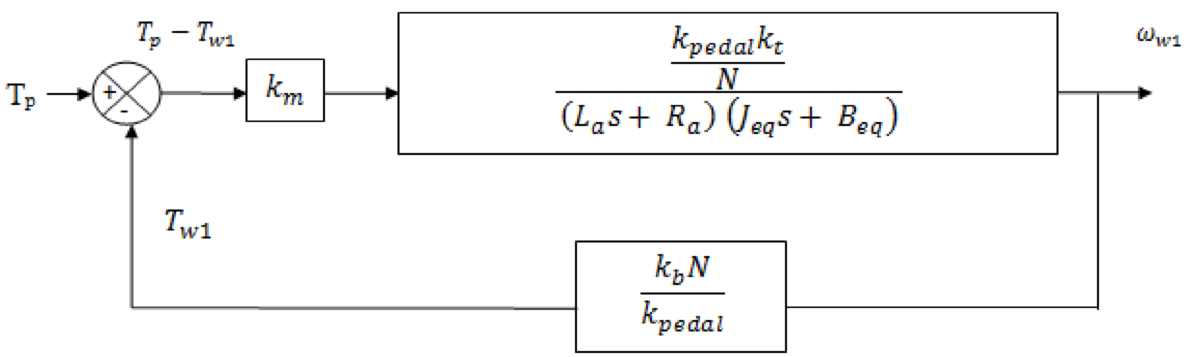

Figure 3.19

d) Transfer function for pedal torque input can be derived from figure 3.17 as following:

$$\frac{\omega_{w1}}{T_p} = \frac{\dfrac{k_m k_{pedal} k_t / N}{(L_a J_{eq})s^2 + (L_a B_{eq} + R_a J_{eq})s + R_a B_{eq}}}{1 + \dfrac{k_m k_{pedal} k_t / N}{(L_a J_{eq})s^2 + (L_a B_{eq} + R_a J_{eq})s + R_a B_{eq}} \dfrac{k_b N}{k_{pedal}}}$$

$$= \frac{\dfrac{k_m k_{pedal} k_t}{N}}{(L_a J_{eq})s^2 + (L_a B_{eq} + R_a J_{eq})s + R_a B_{eq} + k_m k_t k_b}$$

e) Let, $K' = \frac{k_m k_{pedal} k_t}{N}$, then,

$$\frac{\omega_{w1}}{T_p} = \frac{K'}{(L_a J_{eq})s^2 + (L_a B_{eq} + R_a J_{eq})s + R_a B_{eq} + k_m k_t k_b}$$

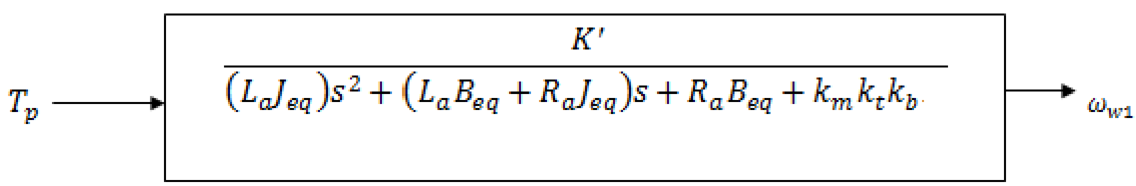

Figure 3.20

2) T_t active, $T_p = 0$

i)

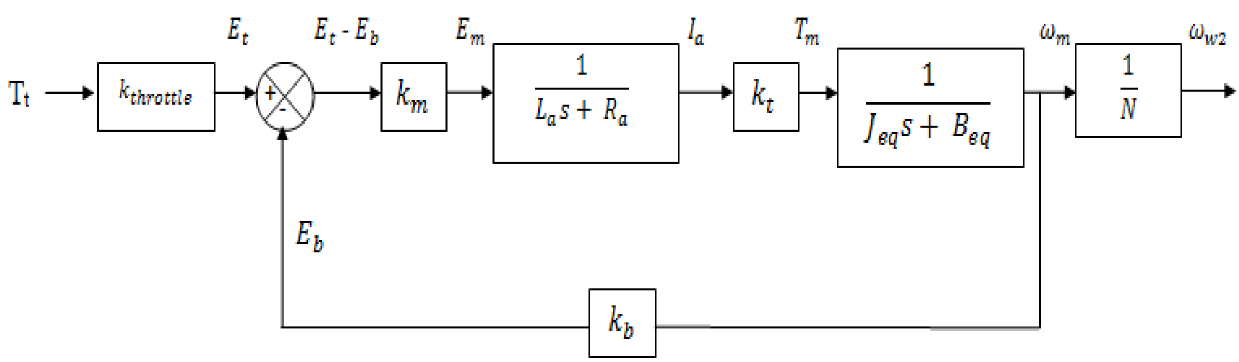

Figure 3.21

ii) Reducing the block diagram in the same procedure,

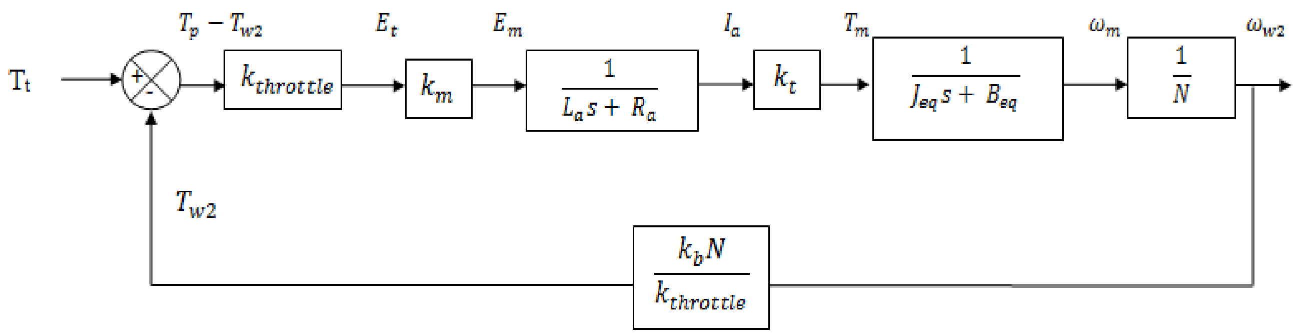

Figure 3.22

iii)

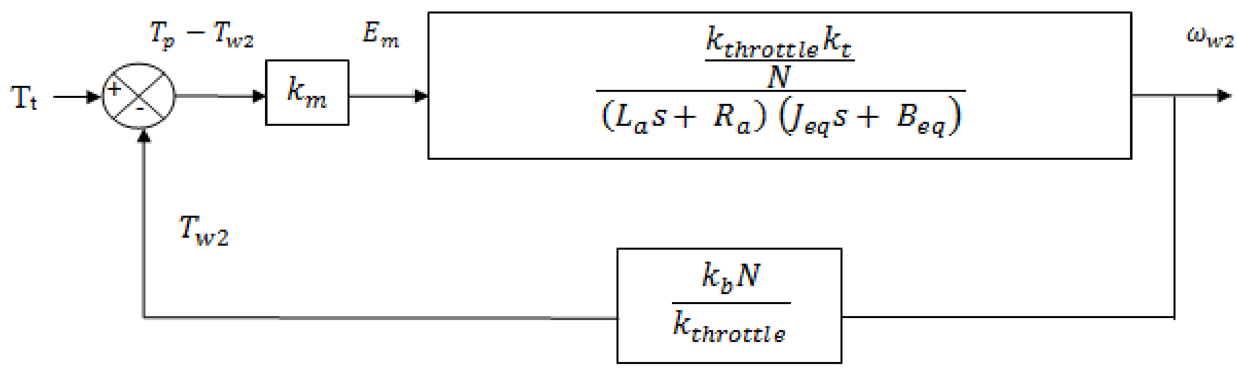

Figure 3.23

iv) Deriving the transfer function in the same way,

$$\frac{\omega_{w2}}{T_t} = \frac{\dfrac{\frac{k_m k_t k_{throttle}}{N}}{(L_a J_{eq})s^2 + (L_a B_{eq} + R_a J_{eq})s + R_a B_{eq}}}{1 + \dfrac{k_m k_{throttle} k_t / N}{(L_a J_{eq})s^2 + (L_a B_{eq} + R_a J_{eq})s + R_a B_{eq}} \dfrac{k_b N}{k_{throttle}}}$$

$$= \frac{k_m k_{throttle} k_t / N}{(L_a J_{eq})s^2 + (L_a B_{eq} + R_a J_{eq})s + R_a B_{eq} + k_m k_t k_b}$$

v) Let $K'' = \frac{k_m k_{throttle} k_t}{N} = k_m \frac{\theta_{tmax}}{N\, k_s E_{in}} k_t$,

then, $\frac{\omega_{w2}}{T_t} = \frac{K''}{(L_a J_{eq})s^2 + (L_a B_{eq} + R_a J_{eq})s + R_a B_{eq} + k_m k_t k_b}$

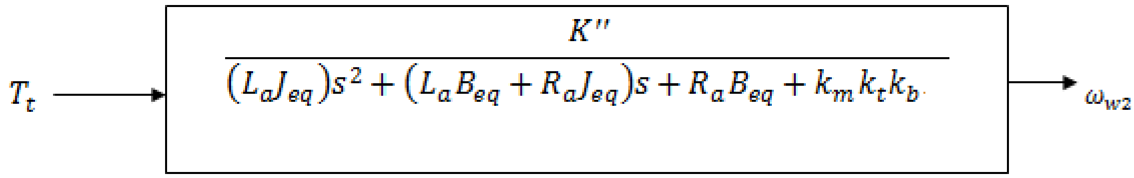

Figure 3.24

Finally the mathematical equation of the full system is:

$$\boldsymbol{\omega_w = \omega_{w1} + \omega_{w2}}$$

$$= \frac{K'}{(L_a J_{eq})s^2 + (L_a B_{eq} + R_a J_{eq})s + R_a B_{eq} + k_m k_t k_b} T_p + \frac{K''}{(L_a J_{eq})s^2 + (L_a B_{eq} + R_a J_{eq})s + R_a B_{eq} + k_m k_t k_b} T_t$$

Where,

$K' = k_m k_{pedal} k_t / N = k_m k_p k_a k_{amp} k_t / N$

$K'' = k_m k_{throttle} k_t / N = k_m \frac{\theta_{tmax}}{N k_s E_{in}} k_t$

$k_m \rightarrow$ Motor amplifier gain

$k_p k_a k_{amp} \rightarrow$ Torque sensor, torque adjustor, LM358 opamp gain accordingly

$k_t \rightarrow$ torque constant

$\theta_{tmax} \rightarrow$ Maximum throttle rotation angle

$k_s E_{in} \rightarrow$ throttle spring constant, throttle input voltage accordingly

N →Gear ratio

3.4 Conclusion

The derived mathematical model depicts that the system is a 2nd order system. During the derivation, all the parameters have been identified and have fixed value except motor amplifier gain. Motor amplifier gain can be varied based on the demand of the amplitude of angular or linear velocity or both. To what extent the gain can be varied has been determined in the following chapter. The parameters are determined and shown in the following table.

Table 3.2: Parameters of the equation

Parameters	Values and units
k_p	0.3
k_a	0.6
k_{amp}	1.26
θ_{tmax}	1.22173 rad
E_{in}	5 V
k_s	0.001 Nm/rad
J_{eq}	27.82 kgm^2
B_{eq}	3.68 Nm/rad/s

Other parameter values were provided in table 1.

For our system, putting the definite values of the identified parameters, the determined transfer function corresponding to the torque sensor input is :

$$\frac{\omega_{w1}}{T_p} = \frac{1.82}{0.003s^2+1.95s+1.1} \quad \text{................(B)}$$

And the transfer function corresponding to the throttle input:

$$\frac{\omega_{w2}}{T_t} = \frac{1960.35}{0.003s^2+1.95s+1.1} \quad \text{................(C)}$$

Chapter 4

System Analysis, MATLAB Simulation and Results

4.1 Introduction

In this chapter, we will try to find the range of motor amplifier gain using several methods. Taking the value between the ranges, we can use any particular gain value for obtaining the desired output. Moreover, system build up in MATLAB , simulation and comparison with real time situation will also be done here. For stability analysis, we used Routh-Hurwitz stability criterion and Root locus. For the relative stability analysis between two input responses, bode plot has been used. The methods used for the system analysis will be discussed broadly in the following sections.

4.2 Range of gain, k_m determination using Root Locus Technique

Root Locus technique is a graphical presentation of the closed loop poles as a system parameter is varied [1]. Analyzing the root locus we understand in which way the parameter gain can be varied and their corresponding transient response and close loop characteristic equation. Root locus plot shows how the closed loop poles vary when the system parameter or gain is changed [8].

4.2.1 Root locus plot for Pedal torque, T_p

Recalling figure 3.19 we can see,

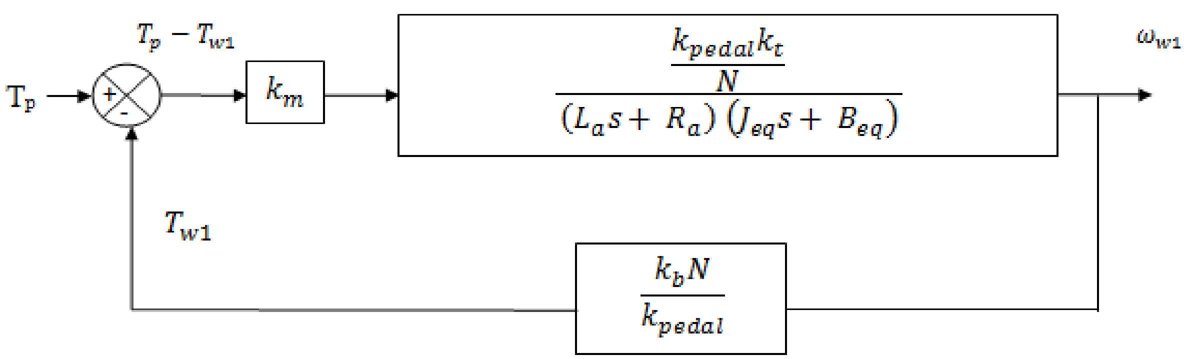

For root locus analysis, we assumed that $k_m$can be varied and it is the close loop gain of the system. Henceforth, the close loop transfer function,

$$\frac{\omega_{w1}}{T_p} = \frac{0.038k_m}{0.003s^2+1.95s+0.26+0.017k_m} \quad \text{....................(D)}$$

Here, close loop gain is k_m

$$G(s) = \frac{\frac{k_t k_{pedal}}{N}}{(L_a J_{eq})s^2+(L_a B_{eq}+R_a J_{eq})s+R_a B_{eq}} = \frac{0.038}{0.003s^2+1.95s+0.26}$$

$$H = \frac{k_b N}{k_{pedd}} = 0.463$$

To find the range of gain, the root locus plot was done using a MATLAB code.

At first for $k_m = 1$, the close loop transfer function for pedal torque becomes,

$$\frac{\omega_{w1}}{T_p} = \frac{0.038}{0.003s^2+1.95s+0.2776}$$

the code for root locus plot is in figure 4.1

```
clear all
clc



k_m=1;

Gnum=0.038;
Gden=[ 0.003 1.95 0.26];
G=tf(Gnum, Gden );

H=0.463;
figure(1)
Pedal=feedback(G*k_m,H)
rlocus (Pedal)
figure(2)
step (Pedal)

```

Figure 4.1 Code for Root Locus Plot with step response

And the result is shown below:

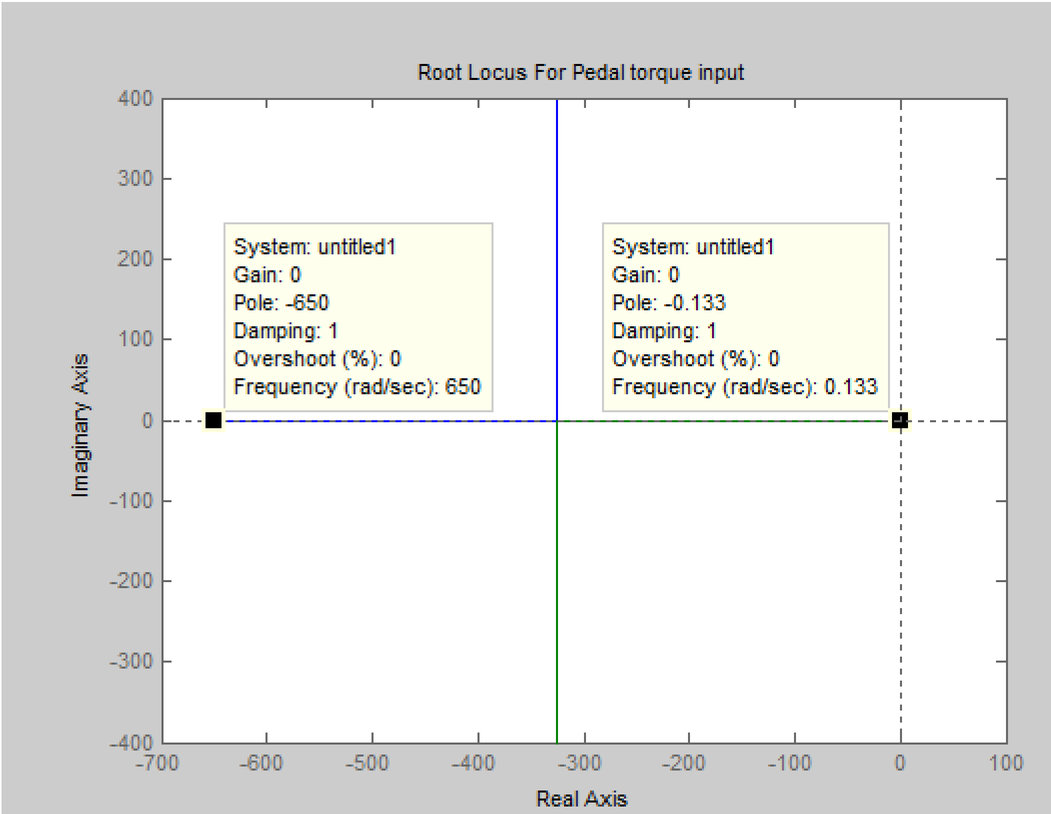

Figure 4.2 Root locus graph for pedal

Analysis from the root locus

In the figure above, the system has demonstrated-

a) Two poles at -650, -0.133.
b) On the poles, the gains are zero. The gain k_m can be varied between two poles.
c) As k_m increases, two roots moves horizontally towards each other and collides at s= -324 and moves away vertically from each other.
d) The path of roots from the starting point -650 is blue that means the roots start from negative real axis at point -650 and ends at infinity through positive imaginary axis. If the path of roots starts from -0.133, the color of path is green and ends at infinity through negative imaginary axis.
e) There are no poles at the right hand side of the s-plane. From the graph, we can come to the decision that the paths of both roots never move to the right hand side of the s- plane but goes to the infinity as displayed on imaginary axis. **The system is inherently stable in case of pedal torque input.**

f) On the real axis, gain can be varied from 4.5-8300

4.2.2 Root locus plot for throttle input, T_t

Recalling the figure 3.23

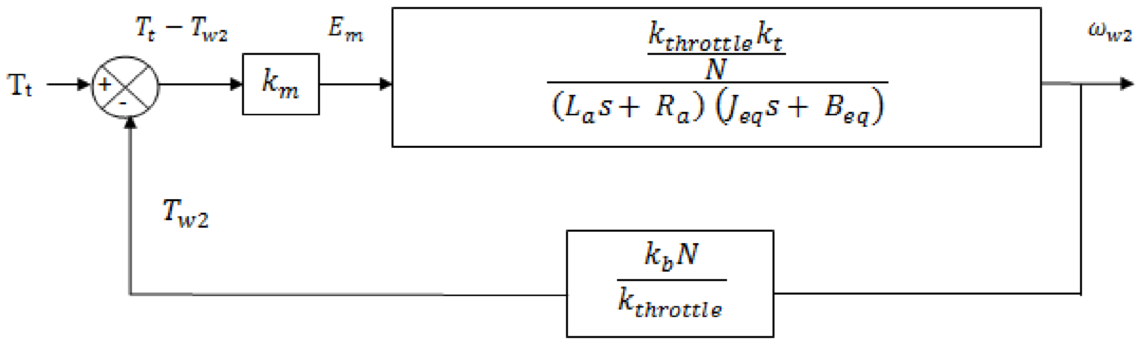

The corresponding transfer function is:

$$\frac{\omega_{w2}}{T_t} = \frac{28.59k_m}{0.003s^2+1.95s+0.26+0.017k_m} \quad \text{.......................(E)}$$

In order to put the values and functions in code,

Here,

$$G(s)=\frac{k_{throttle}k_t/N}{(L_aJ_{eq})s^2+(L_aB_{eq}+R_aJ_{eq})s+R_aB_{eq}+k_mk_tk_b} = \frac{28.59}{0.003s^2+1.95s+0.26}$$

$$H = \frac{k_bN}{k_{throttle}} = 0.00042$$

For $k_m = 1$,

The code is:

```
clear all
clc



k_m=1;

Gnum=28.59;
Gden=[ 0.003 1.95 0.26];
G=tf(Gnum, Gden );
H=0.00042;
figure(1)


Throttle=feedback(G*k_m,H);
figure(2)
step (Throttle)
```

The result of the simulation of this code is as same as Pedal torque one . The path of the two roots' (-650 & -0.14) colliding point has not changed(s=-324) and at the colliding point the gain, k_m is 11.1. The system is inherently stable too for the throttle input.

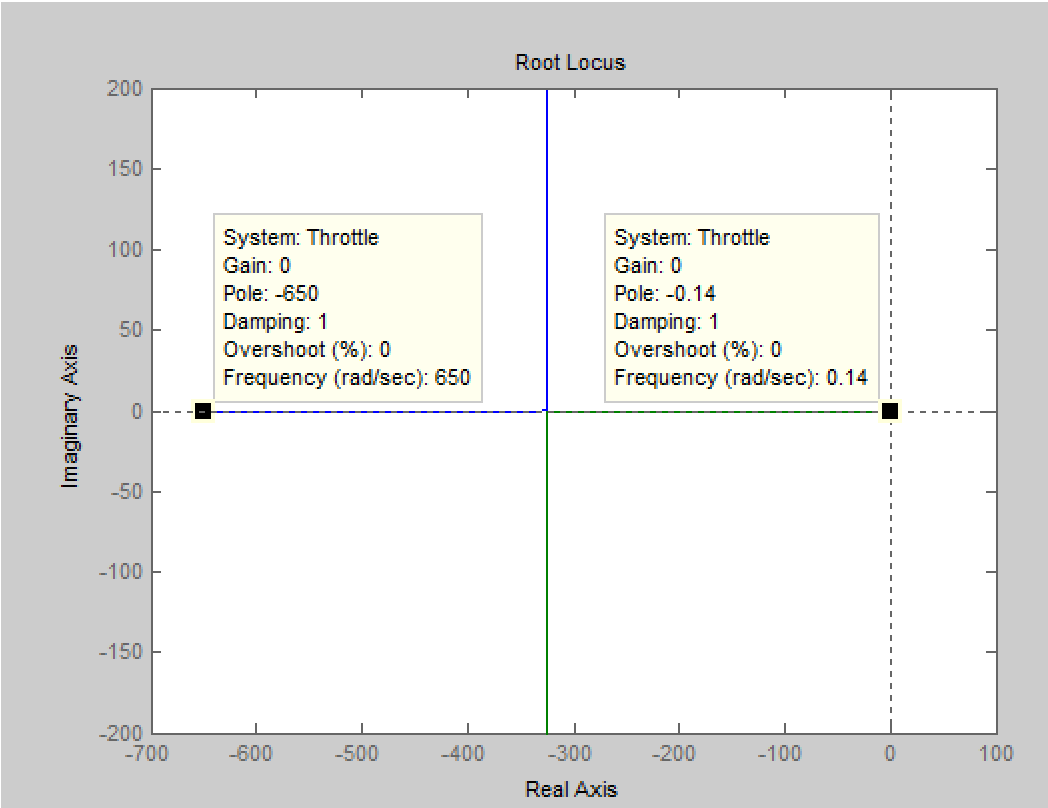

Figure 4.3 Root locus plot for throttle

Since, root locus is only supported for SISO(single input, single output) models in MATLAB , for MISO (multiple input, single output) systems, root locus cannot be done .

```
MISO


Transfer function from input to output...
                0.038
 #1:  --------------------------
      0.003 s^2 + 1.95 s + 0.277

                28.59
 #2:  --------------------------
      0.003 s^2 + 1.95 s + 0.277

??? Error using ==> lti.rlocus at 78
Root locus is only supported for SISO models.
```

Figure 4.4 Error found while performing root locus for MISO system

A question may rise that, why poles have to be on the left hand side of the s-plane to become stable. The answer can be given by a simple example. Consider a system which is $N(s) = \frac{1}{s+b}$, of which inverse laplace transform is e^{-bt}. A pole on the right hand side means the system has a positive real pole. That means 'b' have to be negative to be a pole. Then the system becomes e^{bt} which means the output of the system will exponentially rise with time to the infinity, the system become unstable. Which is why the poles have to be on the left hand side to become stable.

4.3 Step response of the system with variation of gain, k_m

To gain the valuable insight about the system, step response analysis is important. From the root locus, we come to know that gain can be varied between path of poles. From the step response, we can know that what type of system it represents and according to that we can design our models. As the gain k_m varies, the nature of unit response of the system varies. For our system, we will show variation of pole locations with corresponding step response analysis data with plots.

Step Response for Pedal Input:

In figure 4.2 we have seen that the poles of root locus for pedal torque input is -650 and -0.133. From -650 starting point, the path of poles moves from real to positive imaginary axis and from -0.133 starting point, the path of pole moves from real axis to negative imaginary axis.

We will vary the gain accordingly to see if the nature of inputs (such as under damped, overdamped, undamped or critically damped) as well as the response time changes or not.

Before that, we have to understand the terms that we are going to use. The equation for general second order system is,

$$G(s) = \frac{\omega_n^2}{s^2 + 2\xi\omega_n s + \omega_n^2}$$

Where,

ω_n =natural frequency (rad/sec)

ξ =damping ratio.

Natural frequency , ω_n is the frequency of oscillations without damping[1]. These two quantities are the determinants of characteristics of a second order transient response.

If, $\xi > 1$, the system is overdamped.

$\xi = 1$, the system is critically damped.

$\xi < 1$, the system is underdamped.

Other parameters are as follows:

Rise time, T_r: The time required to rise from low value to peak high value of the transient response.

Peak time, T_p: Time required to reach the peak value of the response.

% Overshoot: the amount of which the waveform overshoots the steady state or final value at the peak time is expressed as the percentage of the steady state value [1].

Settling time, T_s: the time required for the transient's damped oscillations to reach and stay within $\pm 2\%$ of the steady state value (Nise,2015).

Example:

For , k_m=1, the transfer function of pedal torque input to wheel angular velocity of our system is, from equation (D) from previous chapter we get,

$$\frac{\omega_{w1}}{T_p} = \frac{0.038k_m}{0.003s^2 + 1.95s + 0.26 + 0.017k_m} = \frac{0.038}{0.003s^2 + 1.95s + 0.277}$$

$$= \frac{12.7}{s^2 + 650s + 92.3}$$

Comparing with the general second order transfer function for transient response,

Here, $\omega_n = \sqrt{(92.3)} = 9.61$

$\xi = \frac{650}{2*9.61}$ =33.82, the system is overdamped. MATLAB shows 1 for the value of zeta. The only way to understand while it is overdamped or not is that the system has real poles (Nise,2015).

The poles of this function are -0.1421, -650.

The unit step response of the system is:

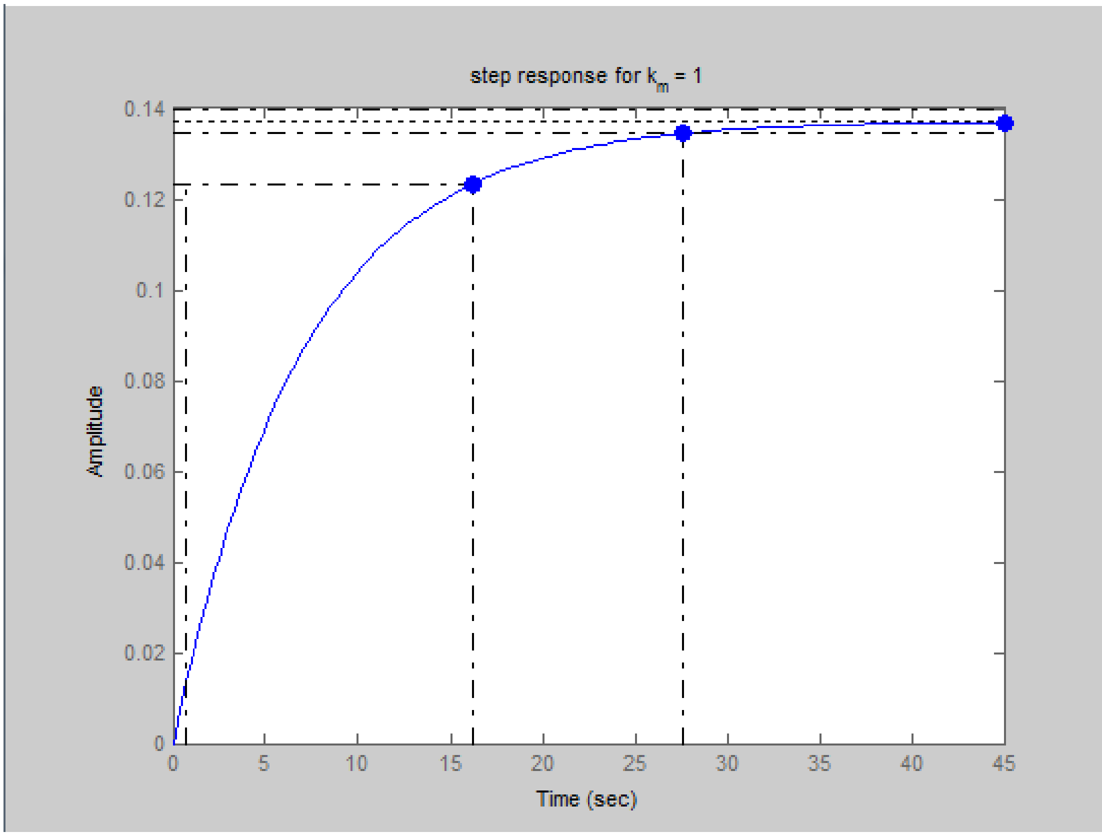

Figure 4.4 Step response for k_m =1

From the graph, we found that,

Rise time: 15.4652

Settling time: 27.5374

Overshoot: 0

Peak: 0.1371

Peak time: 55.0127

The variation of gain (k_m) with corresponding information of step response of the pedal torque is given in the following table:

Table 4.1 Characteristics of step response of the pedal torque input

k_m	Pole 1	Pole 2	ξ	ω_n (rad/s)	T_r (sec)	T_p (sec)	T_s (sec)	%OS	Peak value
1	-0.1421	-649.85	1	9.609	15.47	55.0127	27.5	0	0.1371
10	-0.2206	-649.78	1	11.97	9.96	35.4	17.74	0	0.8834
15	-0.2642	-649.74	1	11.97	8.32	29.58	14.8	0	1.11
20	-0.3078	-649.69	1	14.14	7.1379	25.39	12.71	0	1.2662
40	-0.4824	-649.52	1	17.70	4.5549	16.2	8.11	0	1.62
50	-0.4824	-649.43	1	19.24	3.8567	13.72	6.87	0	1.711
100	-0.5697	-648.99	1	25.56	2.183	7.7644	3.9	0	1.938

As the variable gain increases, the system remains **overdamped** no matter the value is, because we are getting real poles from the equations. The natural frequency increases as the gain increases. The rise time, peak time values also increased in the same way. From this, we can come to a conclusion that the speed of the system increases as we enhance the gain value. One can use a gain value based on the demand of the rise time ,peak time and other parameters.

Step response for throttle input:

In the same way,

For $k_m = 1$, Transfer function for throttle is:

$$\frac{\omega_{w2}}{T_t} = \frac{28.59}{0.003s^2+1.95s+0.277} = \frac{9530}{s^2+650s+92.3}$$

The system is overdamped as the zeta , poles and natural frequency is the same as pedal input, since the denominator is the same for both cases. However, the step response of the system is shown in figure 4.5

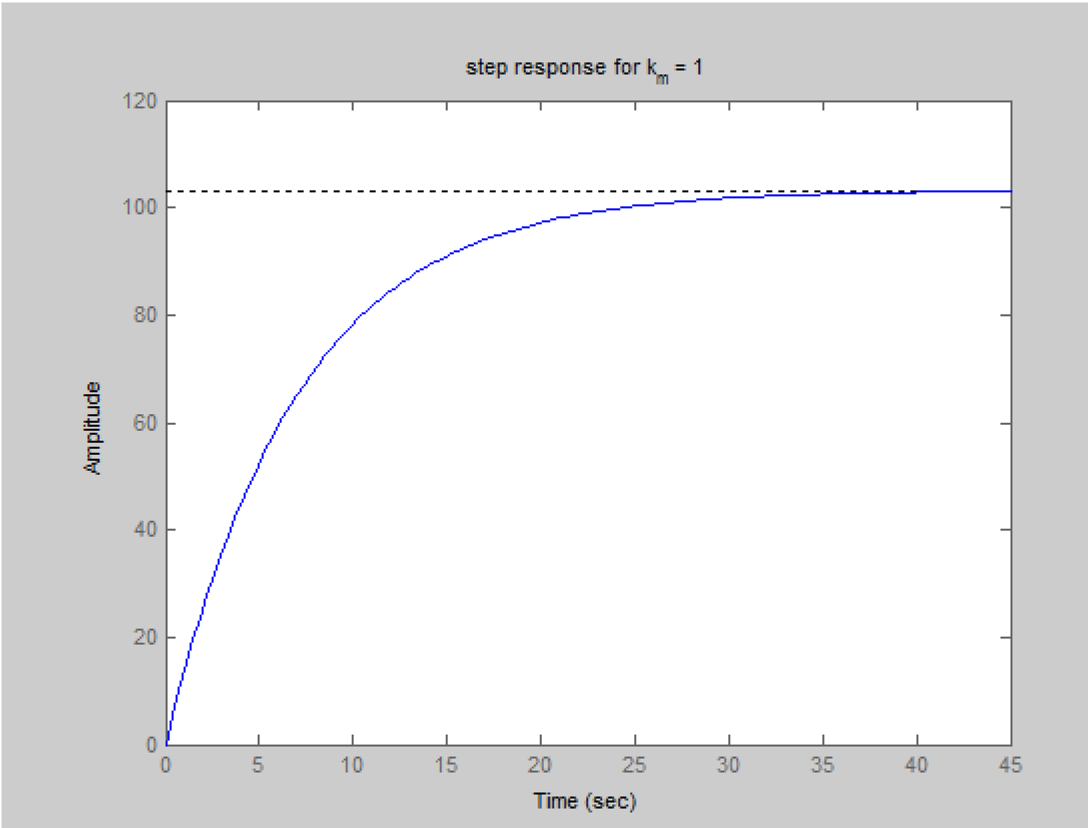

Figure 4.5 Step response for throttle input

The information corresponding to the graph :

Rise time: 15.4652

Settling time: 27.5374

Overshoot: 0

Peak: 103.1714

Peak time: 55.0127

The peak is different but the other parameters are exactly the same as the step response for pedal torque input. Henceforth, zeta, natural frequency and other time parameters does not change while the amplitude of the response increases which can be shown as below:

Table 4.2 Characteristics of step response of the throttle torque input

k_m	Pole 1	Pole 2	ξ	ω_n (rad/s)	T_r (sec)	T_p (sec)	T_s (sec)	%OS	Peak value
1	-0.1421	-649.85	1	9.609	15.47	55.0127	27.5	0	103.17
10	-0.2206	-649.78	1	11.97	9.96	35.4	17.74	0	664.62
15	-0.2642	-649.74	1	13.102	8.32	29.58	14.8	0	832.38
20	-0.3078	-649.69	1	14.14	7.1379	25.39	12.71	0	952.62
40	-0.4824	-649.52	1	17.70	4.5549	16.2	8.11	0	1216.1
50	-0.4824	-649.43	1	19.24	3.8567	13.72	6.87	0	1287.3
100	-0.5697	-648.99	1	25.56	2.183	7.7644	3.9	0	1458.1

As we mentioned before, the peak value rises following the values of gain and other parameters remain unchanged. The system is overdamped for both input responses. If we want to make the system underdamped, then the poles on the root locus will have to be moved vertically from the colliding point of two poles. Then the poles will have complex values the system will be underdamped with damping ratio less than 1.

4.4 Routh-Hurwitz criterion for stability analysis

Routh-Hurwitz criterion can tell us how many poles are in the left or right hand side of the s-plane. But the method does not tell us the location of the poles[1]. However, we just need to check if there are any poles on the right hand side plane. If there are not any poles on the right hand side of the s-plane, then we can say that the system is stable. The beauty of this method is that, using this method, we can also find the unknown parameters of the closed loop system.

The method can be used by (a) generating a data table called routh table and (b) interpreting the Routh table to determine how many poles are on left, right side or on the $j\omega$ axis.

Since Routh table works with the denominator of the transfer function and both of the system (pedal and torque) has same denominator, we can check stability easily. A MATLAB code was written for the Routh table and stability analysis. We used

$k_m = 48$ and that value we will use in MATLAB simulation. Using this value, the polynomial of the denominator in our transfer function will be:

$$0.003s^2 + 1.95s + 1.076 = 0$$

The simulated result of MATLAB code is shown below:

```
input vector of your system coefficients:
 i.e. [an an-1 an-2 ... a0] = [0.003 1.95 1.076]

 Routh-Hurwitz Table:

rhTable =

    0.0030    1.0760
    1.9500         0
    1.0760         0

~~~~~> it is a stable system! <~~~~~

 Number of right hand side poles = 0
Do you want roots of system be shown? Y/N y

 Given polynomial coefficients roots :

sysRoots =

 -649.4477
   -0.5523
```

Figure 4.6 Code generated result for Routh-Hurwitz stability criterion

The number of sign changes (+/-) on the 1st column of the routh table determines how many poles will be on the right hand side. Since there are no sign changes, we can conclude that the system is stable with motor amplifier gain, $k_m = 48$.

4.5 Bode plot analysis of the system

A bode plot is a method of plotting frequency response of LTI systems [9]. In the bode plot of frequency response frequencies in log scale are plotted on the horizontal axis and magnitude in decibel, phase in degrees are on the vertical axis. Bode plot of our system have been done in MATLAB.

Bode plot for pedal input

For bode plot analysis for pedal input, the plot has been shown in figure 4.8 for $k_m = 48$.

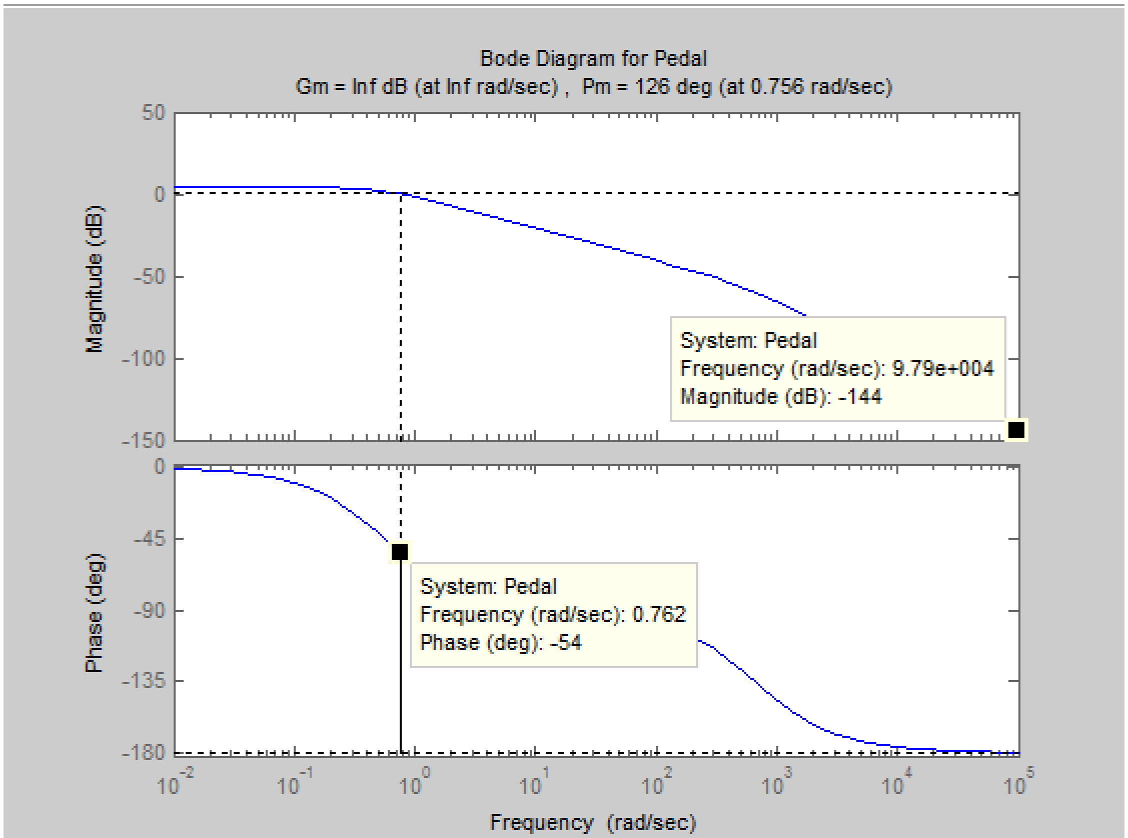

Figure 4.7 Bode plot for pedal

Notice that, gain margin is infinity. That means the plot of phase never crosses the 180 degree line. That also means, the gain value does not matter in the stability analysis of the system. On the other hand, phase margin is 126 degree. Notice that the gain magnitude plot has crossed 0 db line as we can see in the figure. The line that crossed 0 db line (at 0.762 rad/s) is the point which decides the phase margin. At 0.762 rad/s , the phase angle is -54 degree. The difference between that phase angle and 180 degree is the phase margin which is -54-(-180)=126 degree. If the phase angle is 126 degree , the system will be unstable. Furthermore, the system is tolerant of the time delay for the response to the input which will be explained further in the relative stability analysis [10] .

Bode plot for throttle input

The bode plot for throttle input is as follows:

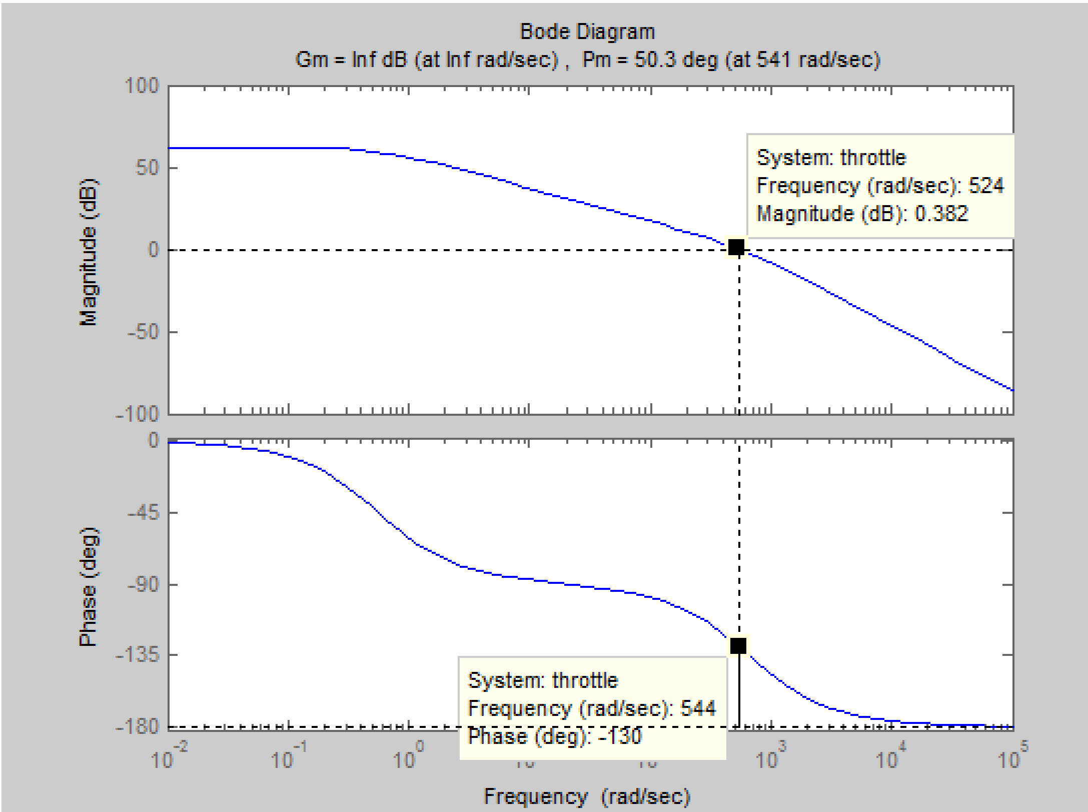

Figure 4.8 Bode plot for throttle response

In the above figure , the gain margin is infinity again. The system can robustly handle the variation of gain for both systems.

The phase margin = -129.7+180= 50.3 degree here.

4.5.1 Relative stability for both inputs:

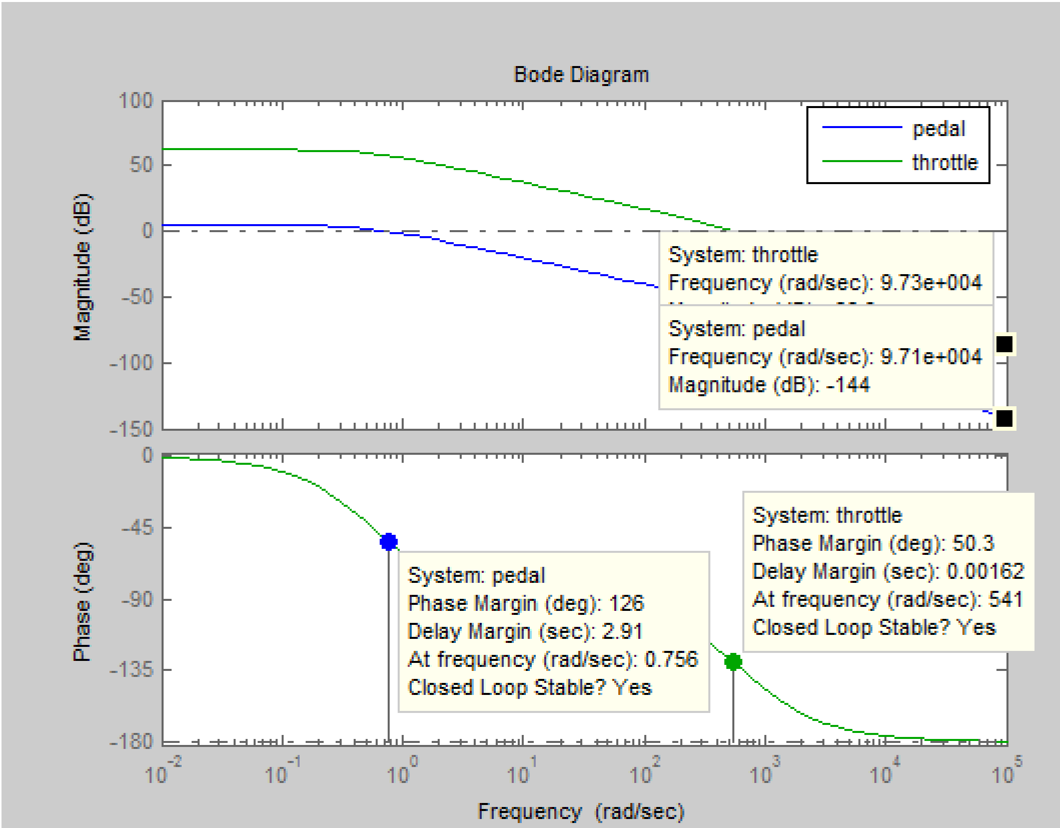

Figure 4.9 Bode plot for both inputs

If the value of the gain increases, the magnitude at end point of gain response for pedal (-144 dB) and throttle (-85.7dB) goes closer to the 0 dB line. In addition to that, the phase margins for both system also decreases following the increment of the gain. To conclude, pedal torque input system is more stable rather than throttle torque input as in the above figure we can see that **the delay margin for pedal torque is 2.91 seconds and for throttle input is 0.00162 seconds. Delay margin means maximum amount of delay time a system can tolerate before the system becomes unstable[11] . In that case, pedal torque input tolerates more time delay than throttle torque. As a result, pedal torque input is more stable than the other system.**

4.6 Simulation in Simulink and results

In Simulink the model of the vehicle was built based on the equation that was found.All the parameters have been identified in previous chapter 3 and 4. Using those values the simulation was done. The simulation was tested with two types of input. One is constant pedal torque input and another is torque sensor output voltage measured during field test of the vehicle by [2].

Simulation using constant pedal torque input and throttle step input

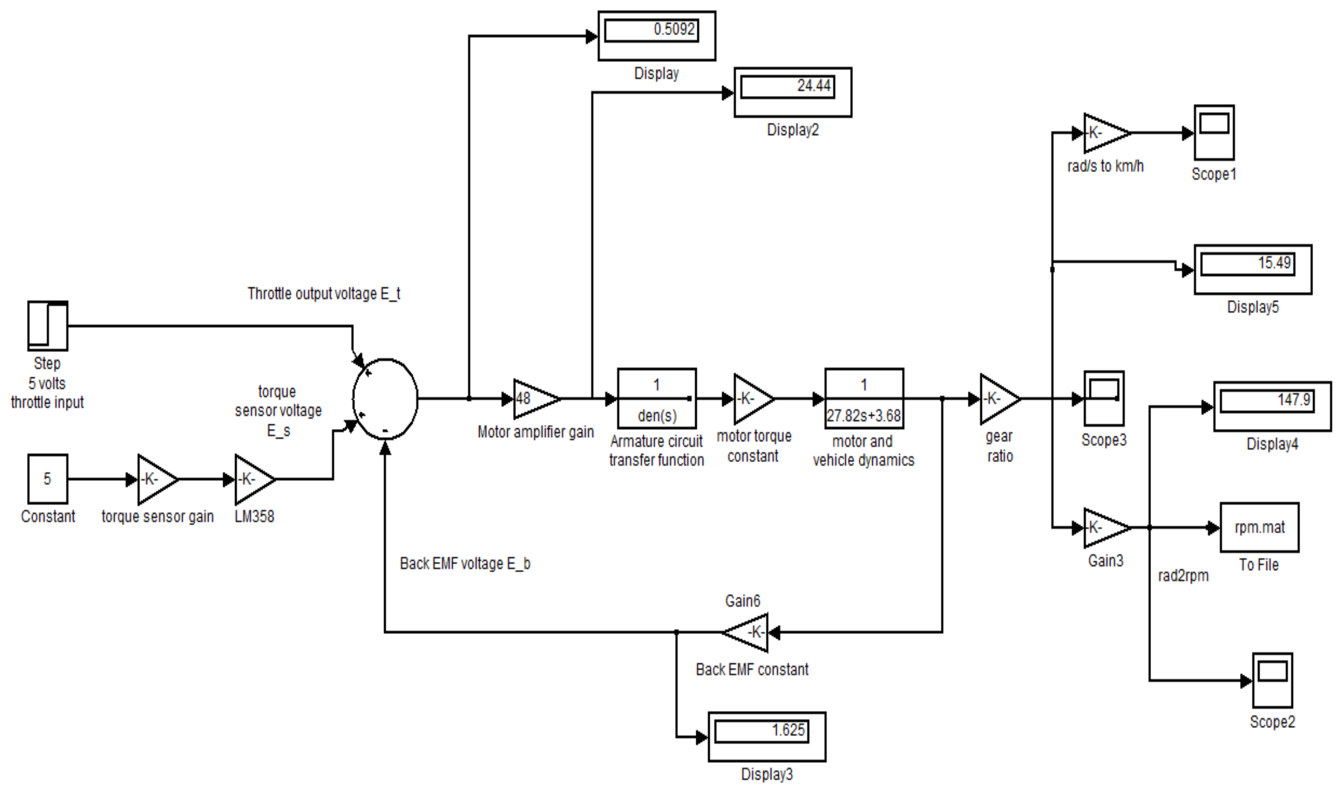

Figure 4.10 Simulink model of the system using constant pedal torque and throttle step input

Corresponding results from the simulation is in the following:

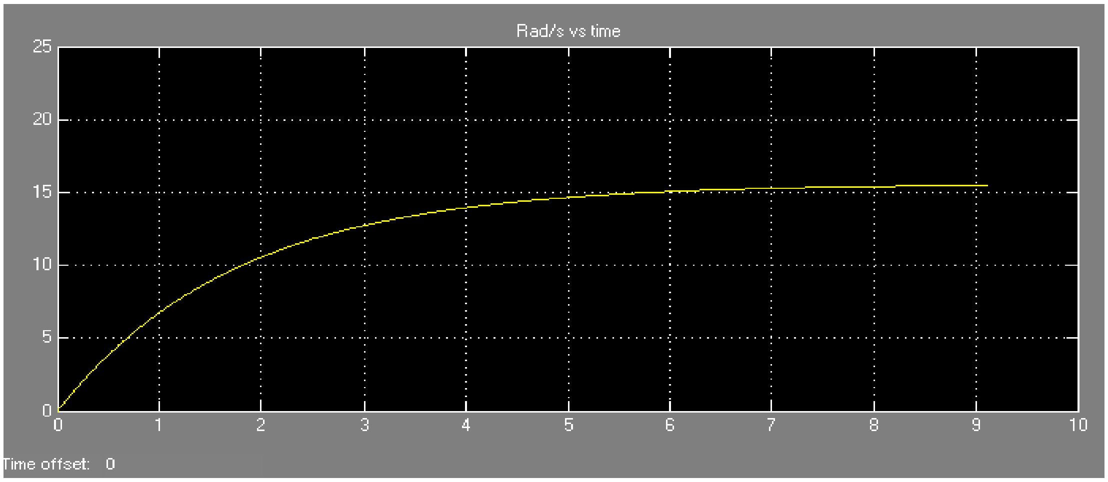

Figure (a)

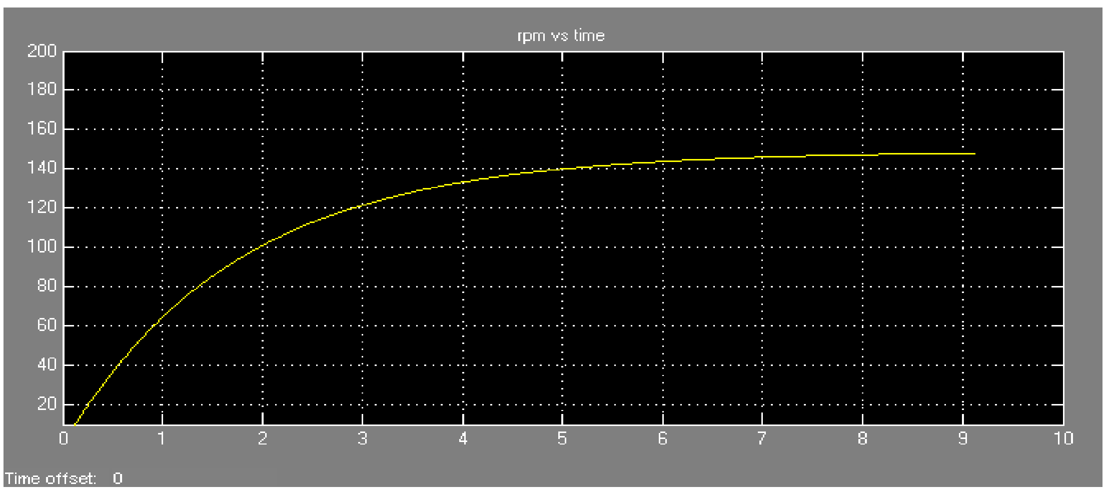

Figure (b)

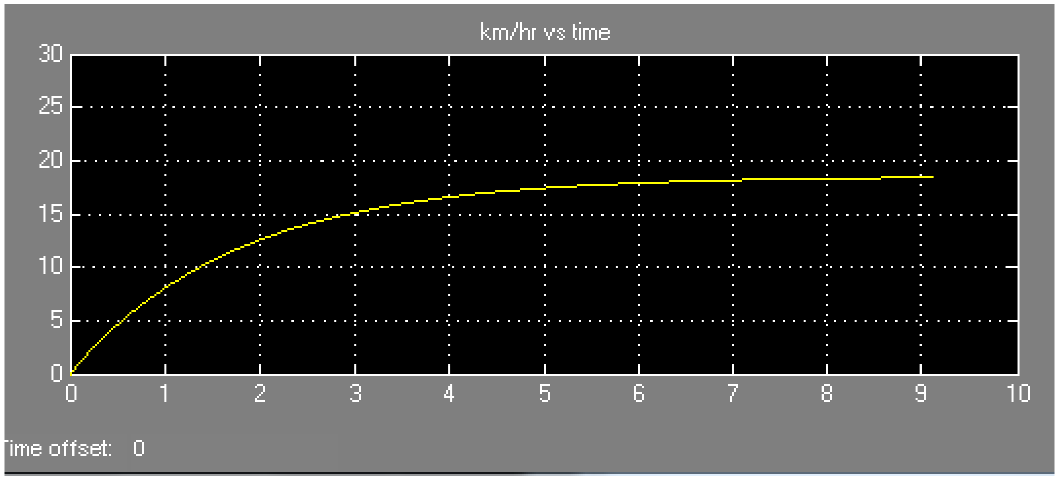

Figure (c)

Figure 4.11 (a) rad/s (b) rpm vs time (c) km/hr graphs , for wheel closed loop angular and linear velocity/time

For unit step throttle input and and constant throttle input the system gives us the result like unit step response. For 15 Nm pedal input and 1 v step throttle, the speed curve shows peak value of 18 km/hr , 150 RPM and 16 rad/s output at steady state.

Simulation using field test data of pedal torque sensor output and unit throttle output:

Simulink model using field test data has been shown in figure 4.13

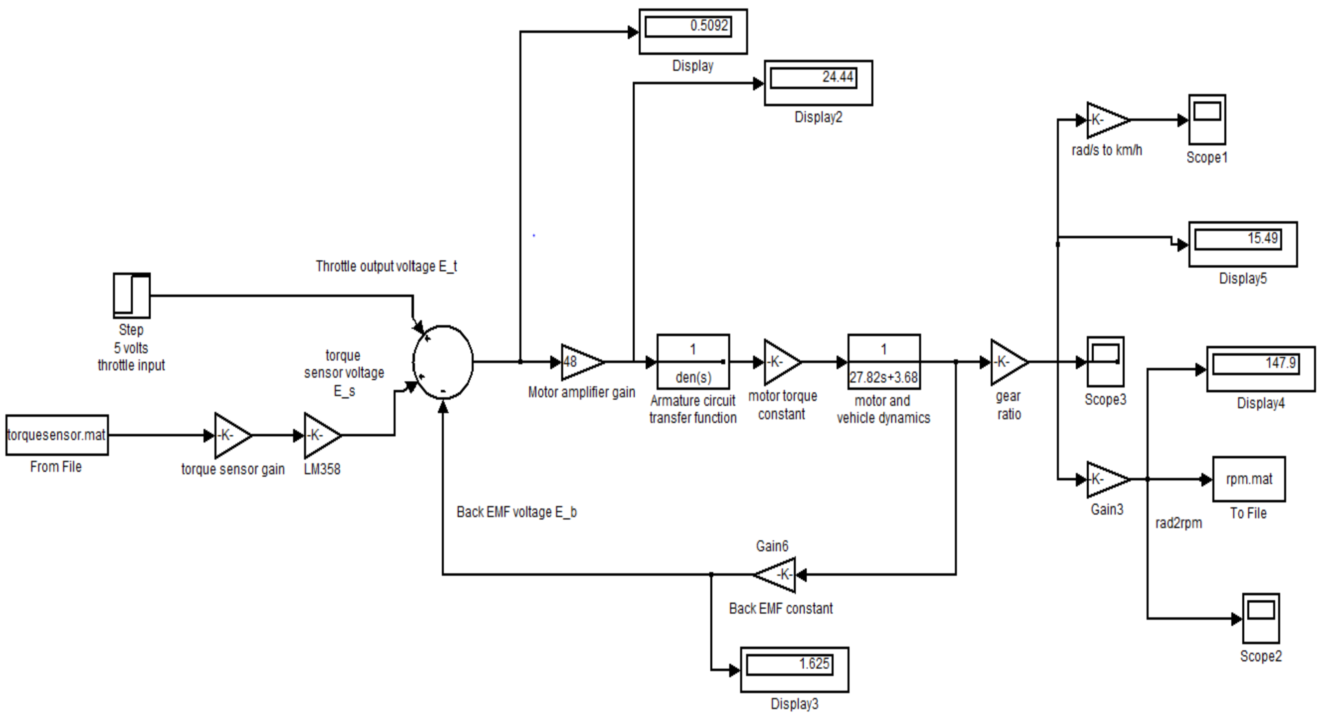

Figure 4.12 Simulink model with field test data of torque sensor output

The data exported to torquesensor.mat file is in the appendix A.

Corresponding graphs of the simulation has been shown in figure 4.13

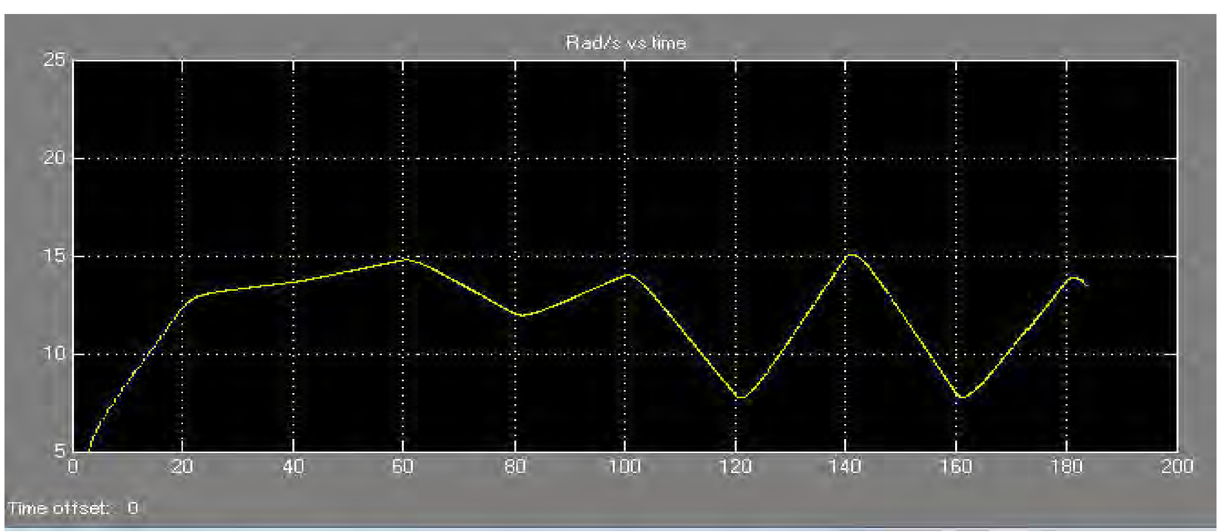

Figure (a)

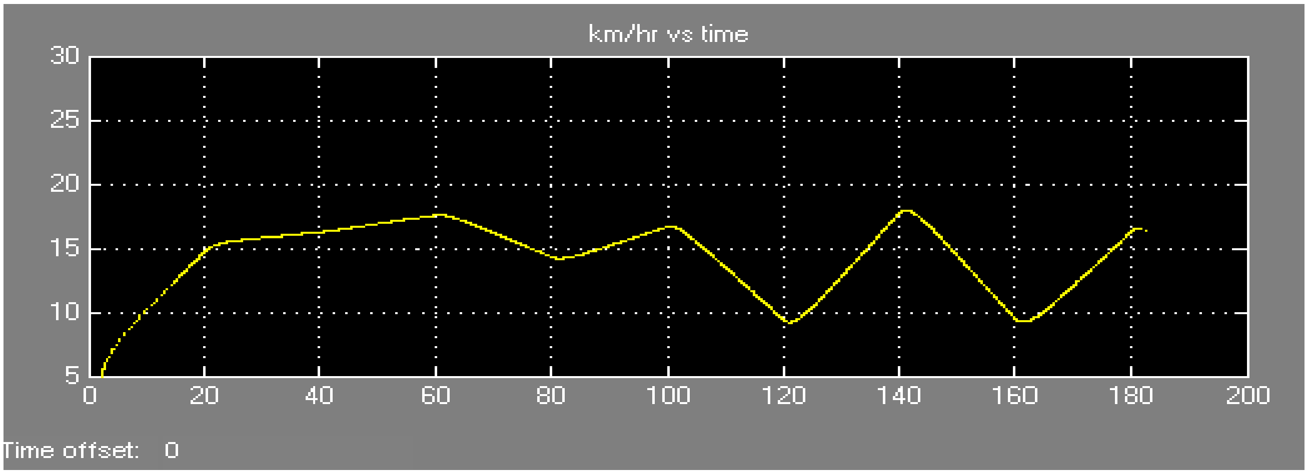

Figure (b)

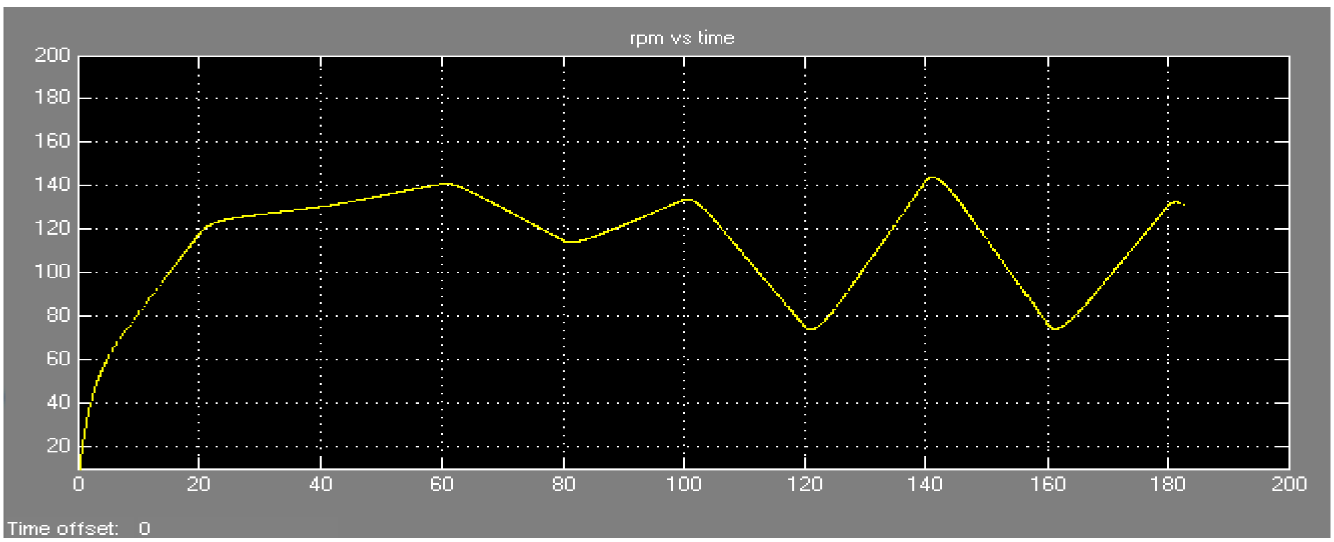

Figure (c)

Figure 4.13 (a)wheel rad/s, (b) vehicle linear km/h, (c) wheel RPM using field test data of pedal torque sensor output

4.7 Conclusion

The simulation using field test data shows that the peak speed is 17.43 km/h and the speed varies due to real time conditions. However, with constant pedal input and step response, the peak speed at the steady state is 18 km/h . The peak value almost matched in both cases.

Chapter 5

Conclusion

The theoretical study of the vehicle was done in order to analyze the system and provide more insight of the functional parameters of the system which can be improved in order to enhance the performance of the vehicle. The developed model is immune to the values of gains and therefore the system is supposed to handle the change of gain robustly.

In bode plot, the phase margin of the gain provided information on how much time delay the system can handle. However, if the gain is increased, the phase margin decreases and the time delay tolerance increases proportionally.

The disturbance torque was not considered in the system due to the unavailability of sufficient lab condition that is necessary to determine certain disturbance, resistive force parameters. It could provide more accuracy to the model.

The model was designed such that according to the demand of the amplitude of the output, damping ratio, type of the system such as underdamped/critically damped or natural frequencies, the model can be configured.

References

[1]N. Nise, *Control systems engineering*, 1st ed. Hoboken, NJ: Wiley, 2015.

[2]F. Khan, A. Aurony, A. Rahman, F. Munira, N. Halim and A. Azad, "Torque sensor based electrically assisted hybrid rickshaw-van with PV assistance and solar battery charging station", *Hdl.handle.net*, 2015. [Online]. Available: http://hdl.handle.net/10361/6967. [Accessed: 09- Apr- 2017].

[3]R. Huq, N. Shuvo, P. Chakraborty and M. Hoque, "Development of Torque Sensor Based Electrically Assisted Hybrid Rickshaw", *Hdl.handle.net*, 2012. [Online]. Available: http://hdl.handle.net/10361/2122. [Accessed: 11- Apr- 2017].

[4]E. Cheever, "Electromechanical Systems", *Lpsa.swarthmore.edu*, 2015. [Online]. Available: http://lpsa.swarthmore.edu/Systems/Electromechanical/SysElectMechSystems.html. [Accessed: 11- Apr- 2017].

[5]C. Abagnale, M. Cardone, P. Iodice, S. Strano, M. Terzo and G. Vorraro, "Derivation and Validation of a Mathematical Model for a Novel Electric Bicycle", 2015. [Online]. Available: http://www.iaeng.org/publication/WCE2015/WCE2015_pp808-813.pdf. [Accessed: 11- Apr- 2017].

[6]2017. [Online]. Available: https://en.nanotec.com/fileadmin/files/Katalog/Nanotec_Catalog_2017.pdf. [Accessed: 11- Apr- 2017].

[7]E. Cheever, "Elements of Rotating Mechanical Systems", *Lpsa.swarthmore.edu*, 2015. [Online]. Available: http://lpsa.swarthmore.edu/Systems/MechRotating/RotMechSysElem.html. [Accessed: 13- Apr- 2017].

[8]E. Cheever, "Why make a root locus plot? - Erik Cheever", *Lpsa.swarthmore.edu*, 2015. [Online]. Available: http://lpsa.swarthmore.edu/Root_Locus/RootLocusWhy.html. [Accessed: 13- Apr- 2017].

[9] 2004. [Online]. Available: http://www.dartmouth.edu/~sullivan/22files/Bode_plots.pdf. [Accessed: 14- Apr- 2017].

[10]"Control Tutorials for MATLAB and Simulink - Introduction: Frequency Domain Methods for Controller Design", *Ctms.engin.umich.edu*, 2017. [Online]. Available: http://ctms.engin.umich.edu/CTMS/index.php?example=Introduction&section=ControlFrequency. [Accessed: 14- Apr- 2017].

[11]S. Ayasun, U. Eminoğlu and Ş. Sönmez, "Computation of Stability Delay Margin of Time-Delayed Generator Excitation Control System with a Stabilizing Transformer", 2014. .

APPENDIX A

Table A : torque sensor input to the system with respect to time

Time (seconds)	Torque sensor input (voltage)
5	0
20	1.03
40	1.16
60	1.37
80	0.81
100	1.25
120	0
140	1.5
160	0
180	1.27
200	0
220	1.48
240	0
260	0
280	1.1
300	1.22
320	1.71
340	0
360	1.53
380	1.14
400	1.5
420	0.66
440	1.97
460	0
480	0.97
500	1.27
520	0
540	1.17
560	1.59
580	1.51
600	1.15
620	1.68
640	1.8
660	1.7
680	1.32

700	1.69
720	1.61
740	0.72
760	0
780	1.12
800	1.55
820	1.55
840	1.14
860	1.34
880	2.03
900	1.82
920	1.04
940	1.86
960	1.17
980	1.48
1000	1.81
1020	1.35
1040	1.73
1060	1.7
1080	0
1100	1.77
1120	0
1140	1.3
1160	0
1180	1.14
1200	0.97
1220	1.32
1240	1.4
1260	1.91
1280	0
1300	1.64
1320	1.89
1340	1.05
1360	1.94
1380	0
1400	0
1420	0
1440	1.54
1460	1.86
1480	1.84

1500	0.86
1520	1.91
1540	0.89
1560	1.5
1580	1.53
1600	1.59
1620	1.42
1640	1.89
1660	0.79
1680	1.54
1700	0.86
1720	0.91
1740	1.54
1760	1.86
1780	1.59
1800	1.42
1820	1.89
1840	1.13
1860	1.54
1880	1.42
1900	1.86
1920	1.54
1940	1.59
1960	0.89
1980	0.89
2000	1.84
2020	1.54
2040	0.86
2060	1.91
2080	1.53
2100	0.79
2120	1.42
2140	1.86
2160	1.84
2180	1.54
2200	0.86
2220	0.89
2240	0
2260	0.79
2280	1.54

2300	1.59
2320	0.89
2340	0.89
2360	1.5
2380	1.54
2400	0.86
2420	0.79
2440	1.84
2460	1.97
2480	1.37
2500	1.68
2520	1.56
2540	1.46
2560	1.43
2580	1.2
2600	1.52
2620	0
2640	1.83
2660	1.57
2680	1.25
2700	1.64
2720	1.77
2740	0.95
2760	1.56
2780	1.47
2800	1.52
2820	1.58
2840	1.83
2860	0
2880	1.37
2900	1.68
2920	1.56
2940	0
2960	1.59
2980	0.89
3000	0.89
3020	1.5
3040	1.54
3060	1.64
3080	0

3100	0.95
3120	0.86
3140	0.79
3160	1.45
3180	1.39
3200	1.83
3220	1.32
3240	1.19
3260	1.69
3280	1.75
3300	1.69
3320	0
3340	1.57
3360	1.12
3380	1.79
3400	1.95
3420	1.75
3440	1.45
3460	1.84
3480	1.3
3500	1.2
3520	1.03
3540	1.47
3560	0
3580	1.31
3600	1.6
3620	1.46
3640	0.9
3660	1.72
3680	1.38
3700	1.53
3720	1.63
3740	1.4
3760	0
3780	1.39
3800	1.3
3820	1.43
3840	0
3860	1.23
3880	1.4

3900	0.84
3920	1.38
3940	1.53
3960	1.63
3980	1.4
4000	1.1
4020	1.39
4040	1.47
4060	1.57
4080	1.12
4100	1.79
4120	1.95
4140	1.75
4160	1.6
4180	1.46
4200	0.9
4220	1.72
4240	1.1
4260	1.08
4280	0.9
4300	1.18
4320	1.34
4340	1.69
4360	1.22
4380	1.43
4400	1.1
4420	1.12
4440	1.2
4460	1.88
4480	1.1